Chapter 20

d-block metal chemistry:

coordination complexes

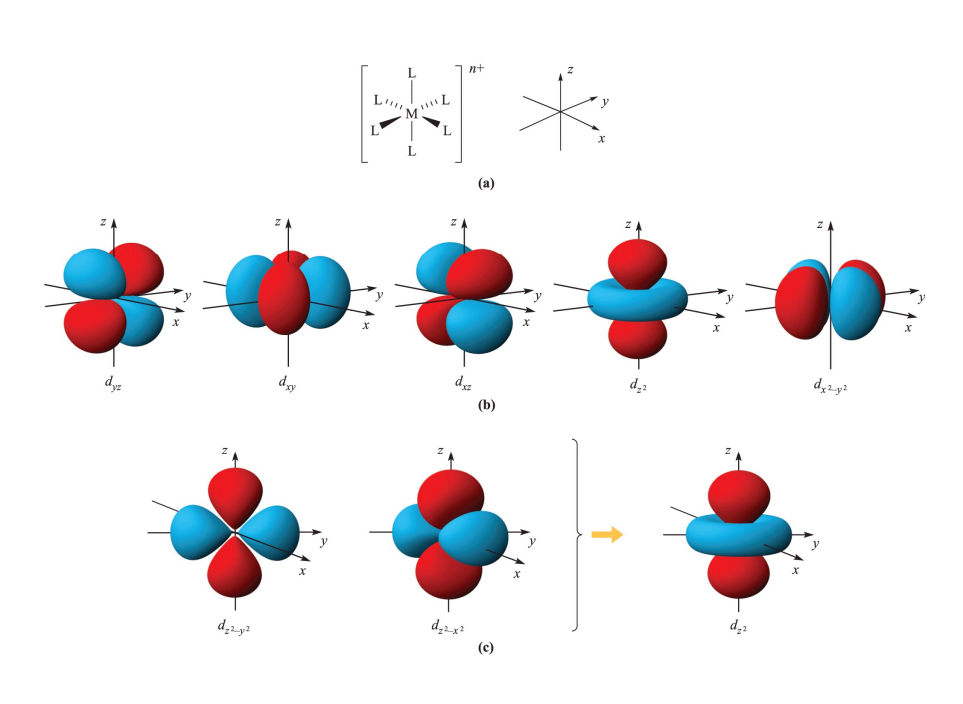
Bonding: valence bond, crystal field theory, MO

Spectrochemical series

Crystal field stabilization energy (CFSE)

Electronic Spectra

Magnetic Properties



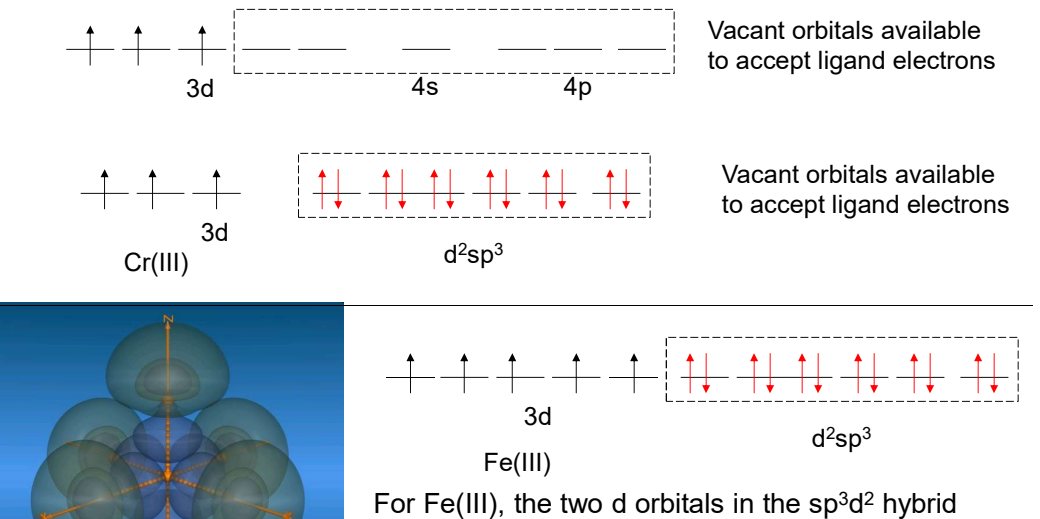
five d-orbitals and the shapes

Hybridization schemes for the σ -bonding frameworks of different geometrical configurations

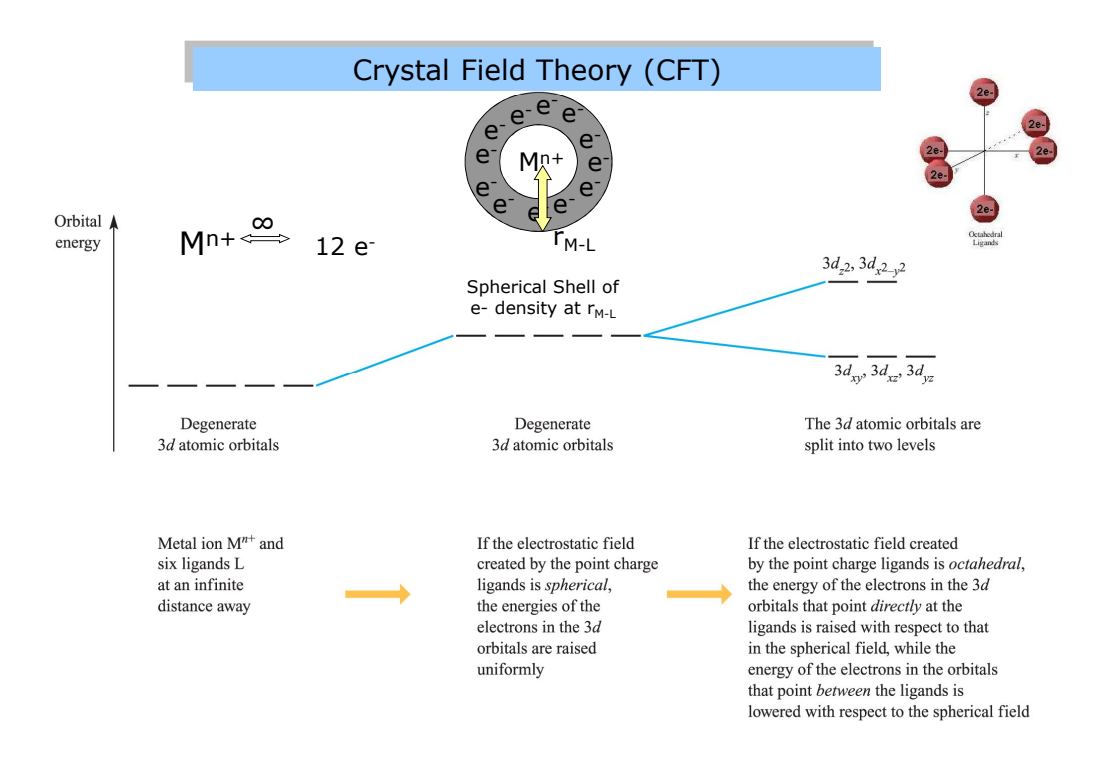
Coordination number	Arrangement of donor atoms	Orbitals hybridized	Hybrid orbital description	Example
2	Linear	s, p_z	sp	$[Ag(NH_3)_2]^+$
3	Trigonal planar	s, p_x, p_y	sp^2	$[HgI_3]^-$
4	Tetrahedral	s, p_x, p_y, p_z	sp^3	$[FeBr_4]^{2-}$
4	Square planar	$s, p_x, p_y, d_{x^2-y^2}$	sp^2d	$[Ni(CN)_4]^{2-}$
5	Trigonal bipyramidal	$s, p_x, p_y, p_z, d_{z^2}$	sp^3d	$[CuCl_5]^{3-}$
5	Square-based pyramidal	$s, p_x, p_y, p_z, d_{x^2-y^2}$	sp^3d	$[Ni(CN)_{5}]^{3-}$
6	Octahedral	$s, p_x, p_y, p_z, d_{z^2}, d_{x^2-y^2}$	sp^3d^2	$[Co(NH_3)_6]^{3+}$
6	Trigonal prismatic	$s, d_{xy}, d_{yz}, d_{xz}, d_{z^2}, d_{x^2-y^2}$	sd^5	$[ZrMe_6]^{2-}$
		or $s, p_x, p_y, p_z, d_{xz}, d_{yz}$	sp^3d^2	
7	Pentagonal bipyramidal	$s, p_x, p_y, p_z, d_{xy}, d_{x^2-y^2}, d_{z^2}$	sp^3d^3	$[V(CN)_7]^{4-}$
7	Monocapped trigonal prismatic	$s, p_x, p_y, p_z, d_{xy}, d_{xz}, d_{z^2}$	sp^3d^3	$[NbF_{7}]^{2-}$
8	Cubic	$s, p_x, p_y, p_z, d_{xy}, d_{xz}, d_{yz}, f_{xyz}$	sp^3d^3f	$[PaF_{8}]^{3-}$
8	Dodecahedral	$s, p_x, p_y, p_z, d_{z^2}, d_{xy}, d_{xz}, d_{yz}$	sp^3d^4	$[Mo(CN)_8]^{4-}$
8	Square antiprismatic	$s, p_x, p_y, p_z, d_{xy}, d_{xz}, d_{yz}, d_{x^2-y^2}$	sp^3d^4	$[TaF_8]^{3-}$
9	Tricapped trigonal prismatic	$s, p_x, p_y, p_z, d_{xy}, d_{xz}, d_{yz}, d_{z^2}, d_{z^2-y^2}$	sp^3d^5	$[ReH_9]^{2-}$

3

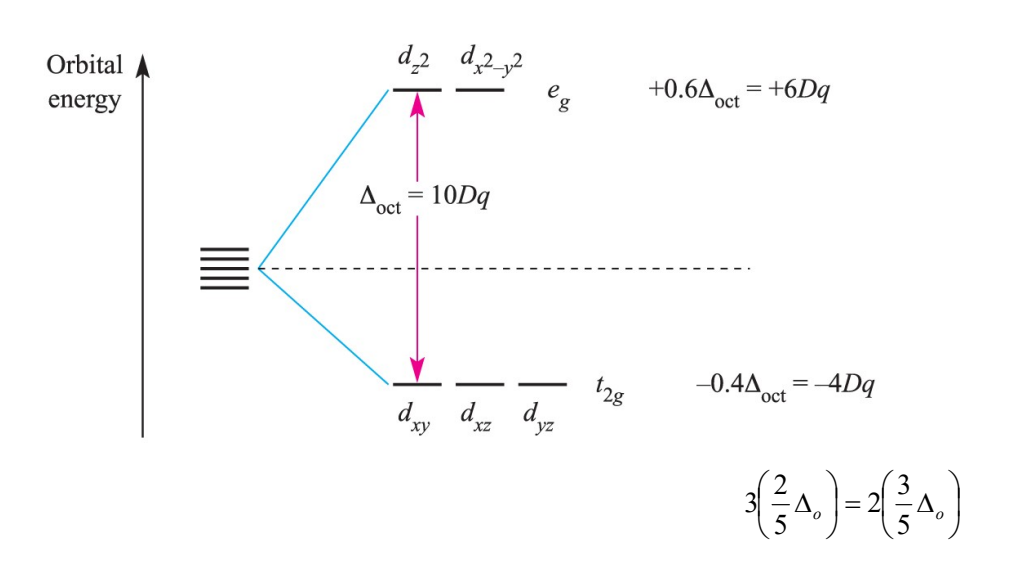
Limitations of VB Theory

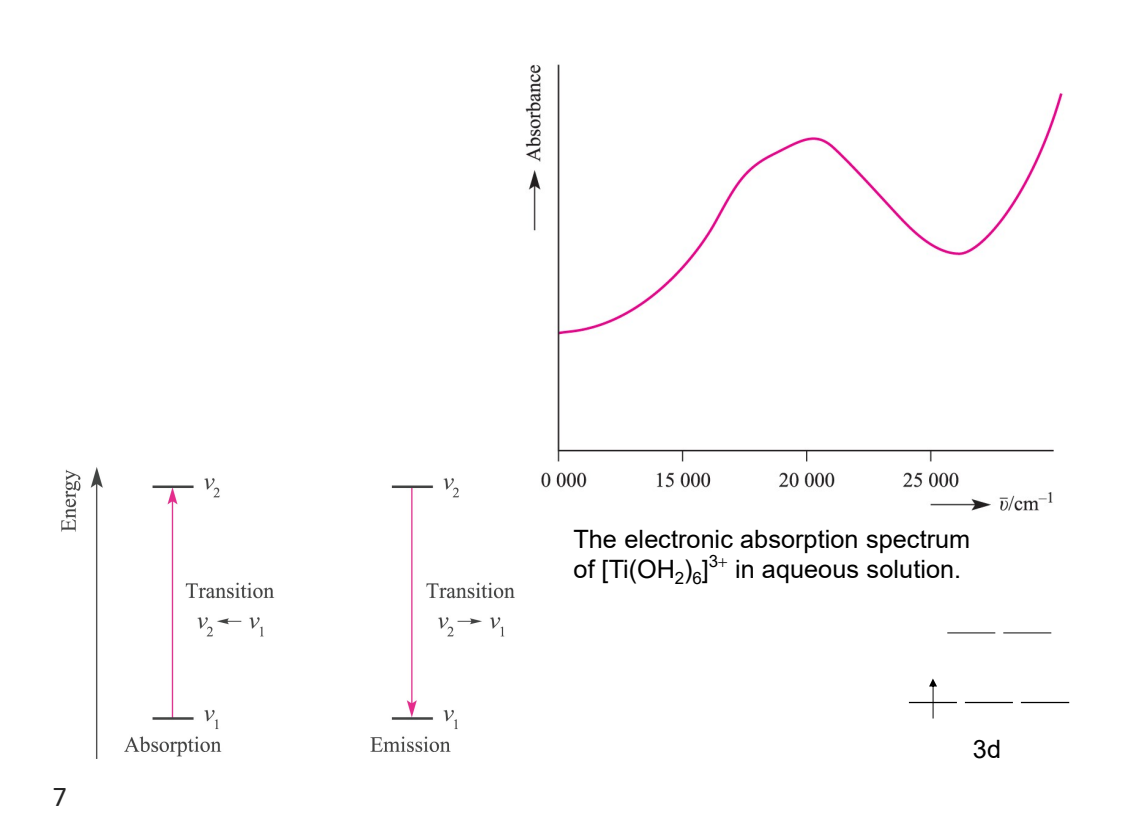


For Fe(III), the two d orbitals in the sp³d² hybrid orbitals would need to be from the 4d orbitals, which is not favorable because the 4d orbitals are much higher in energy than the 3d orbitals.



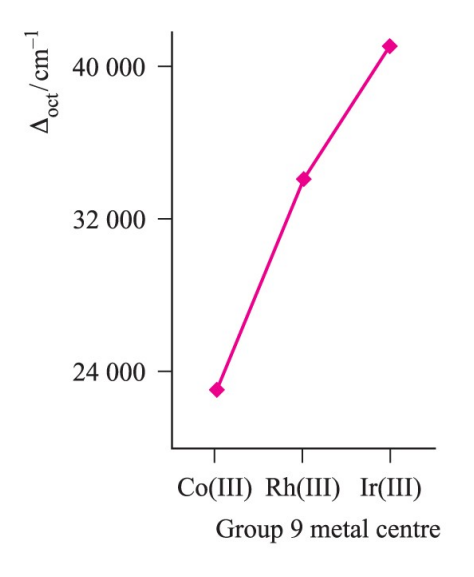
Crystal Field Stabilization Energy (CFSE)





Complex	Δ / cm $^{-1}$	Complex	Δ/cm^{-1}
$[\mathrm{TiF_6}]^{3-}$	17 000	$[\mathrm{Fe}(\mathrm{ox})_3]^{3-}$	14 100
$\left[\mathrm{Ti}(\mathrm{OH_2})_6\right]^{3+}$	20 300	$[Fe(CN)_6]^{3-}$	35 000
$[V(OH_2)_6]^{3+}$	17 850	$[Fe(CN)_6]^{4-}$	33 800
$[V(OH_2)_6]^{2+}$	12 400	$[CoF_{6}]^{3-}$	13 100
$[CrF_6]^{3-}$	15 000	$[Co(NH_3)_6]^{3+}$	22 900
$[Cr(OH_2)_6]^{3+}$	17 400	$[Co(NH_3)_6]^{2+}$	10 200
$[Cr(OH_2)_6]^{2+}$	14 100	$[Co(en)_3]^{3+}$	24 000
$[Cr(NH_3)_6]^{3+}$	21 600	$[Co(OH_2)_6]^{3+}$	18 200
$[Cr(CN)_6]^{3-}$	26 600	$[\mathrm{Co}(\mathrm{OH_2})_6]^{2+}$	9 300
$[MnF_6]^{2-}$	21 800	$[Ni(OH_2)_6]^{2+}$	8 500
$[Fe(OH_2)_6]^{3+}$	13 700	$[Ni(NH_3)_6]^{2+}$	10800
$[Fe(OH_2)_6]^{2+}$	9 400	$[Ni(en)_3]^{2+}$	11 500

Values of $\Delta_{\rm oct}$ for some *d*-block metal complexes.



The trend in values of Δ_{oct} for the complexes [M(NH₃)₆]³⁺ where M = Co, Rh, Ir.

Field strength increases as one proceeds down a column.

$$\frac{\Delta_{\text{oct}}}{\text{Mn(II)} < \text{Ni(II)} < \text{Co(II)} < \text{Fe(II)} < \text{Cr(III)} < \text{Co(III)} < \text{Ru(III)} < \text{Mo(III)} < \text{Rh(III)} < \text{Pd(II)} < \text{Ir(III)} < \text{Pt(IV)}$$

9

Factors affecting the CFSE

First, note that the pairing energies for first-row transition metals are relatively constant.

Therefore, the difference between strong- and weak-field, or low and high- spin cases comes down to the magnitude of the crystal field splitting energy (Δ).

<u>1. Geometry</u> is one factor, Δ_{o} is larger than Δ_{t}

In almost all cases, the Δ_t is smaller than P (pairing energy), so...

Tetrahedral complexes are always weak-field (high spin)

Square planar complexes may either be weak- or strong-field.

2. Oxidation State of Metal Cation -

A greater charge on cation results in a greater magnitude of Δ

Why? A greater charge pulls ligands more strongly towards the metal, therefore influences the splitting of the energy levels more.

3. Size of the Metal Cation -

For second and third-row transition metal ions, Δ_0 is larger than first-row.

Less steric hindrance between the ligands – better overlap w/orbitals.

What are the other factors affecting the CFSE?

4. Identity of the ligands.

A spectrochemical series has been developed and sorted by the ability to split metal d-orbitals.

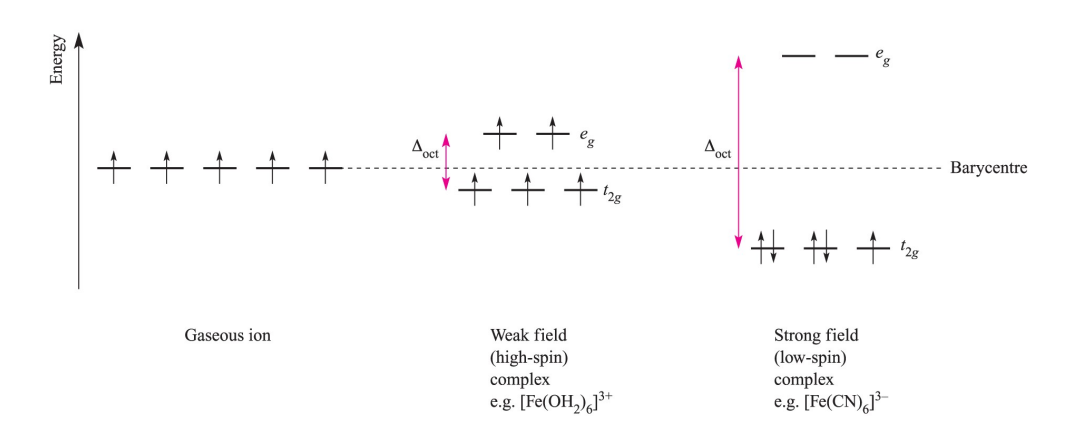
```
I^- < Br^- < S^{2-} < Cl^- < SCN^- < NO_3^- < N^{3-} < F^- < OH^- < C_2O_4^{2-} < H_2O < NCS^- < CH_3CN < py (pyridine) < NH_3 < en (ethylenediamine) < bipy (2,2'-bipyridine) < <math>NO_2^- < PPh_3 < CN^- < CO
```

As the ligands decrease in size, their ability to split the d-orbitals increases. The larger and bulkier ligands exhibit more steric hindrance and approach the metal less effectively.

One might expect that ligands with a negative charge might split the d-orbitals better, but this is not always the case. Notice that water is higher in the series than OH-, even though O on OH- has a high concentration of charge.

The dipole moment of H_2O is larger than NH_3 , but NH_3 is higher in the series. PPh_3 is high in the series, but also very bulky, neutral and has a small dipole moment.

11



Occupation of the 3*d* orbitals in weak and strong field Fe^{3+} (g^{5}) complexes.

$$CFSE = \Delta E = E_{ligand \ field} - E_{isotropic \ field}$$

d^n	High-spin = weak field		Low-spin = strong field		
	Electronic configuration	CFSE	Electronic configuration	CFSE	
d^1	$t_{2g}^{1}e_{g}^{0}$	$-0.4\Delta_{\rm oct}$			
d^2	$t_{2g}^{2}e_{g}^{0}$	$-0.8\Delta_{\mathrm{oct}}$			
d^3	$t_{2g}^{3}e_{g}^{0}$	$-1.2\Delta_{\rm oct}$			
d^4	$t_{2g}^{3}e_{g}^{1}$	$-0.6\Delta_{\rm oct}$	$t_{2g}^{4}e_{g}^{0}$	$-1.6\Delta_{ m out}+P$	
d^5	$t_{2g}^{3}e_{g}^{2}$	0	$t_{2g}^{5}e_{g}^{0}$	$-2.0\Delta_{\rm oct} + 2P$	
d^6	$t_{2g}^{4}e_{g}^{2}$	$-0.4\Delta_{\rm oct}$	$t_{2g}^{6}e_{g}^{0}$	$-2.4\Delta_{\rm oct} + 2P$	
d^7	$t_{2g}^{5}e_{g}^{2}$	$-0.8\Delta_{\rm oct}$	$t_{2g}^{6}e_g^{1}$	$-1.8\Delta_{\mathrm{oct}} + P$	
d^8	$t_{2g}^{6}e_{g}^{2}$	$-1.2\Delta_{\rm oct}$			
d^9	$t_{2g}^{6}e_g^{3}$	$-0.6\Delta_{\rm oct}$			
d^{10}	$t_{2g}^{6}e_{g}^{4}$	0			

Octahedral crystal field stabilization energies (CFSE) for d^n configurations; pairing energy, P, terms are included where appropriate

High Spin : $\Delta_o < P$ Low Spin : $\Delta_o > P$

13

Pairing energies for some 3d metal ions*

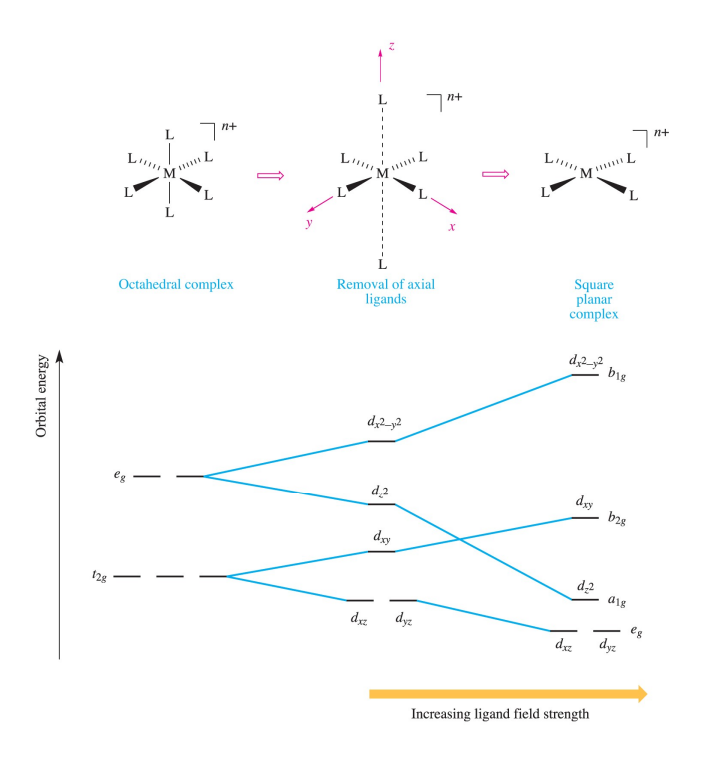
		P (cm ⁻¹)
d ⁴	Cr ²⁺	20,425
	Mn³+	25,215
d^5	Cr+	17,687
	Mn ²⁺	23,825
	Fe ³⁺	29,875
d^6	Mn+	14,563
	Fe ²⁺	19,150
	Co ³⁺	23,625
d^7	Fe⁺	17,680
	Co ²⁺	20,800

Using these pairing energy data and $\Delta_{\text{O}},$ determine if the following complexes are predicted to be high spin or low spin.

- a) $[Fe(OH_2)_6]^{2+}$
- b) $[Fe(CN)_6]^{4-}$

^{*}Pairing energy values refer to free ion, and may be 15-30% smaller for the complexed ion. Orgel, L.E. J. Chem. Phys. **1955**, *23*, 1819.

Square Planar

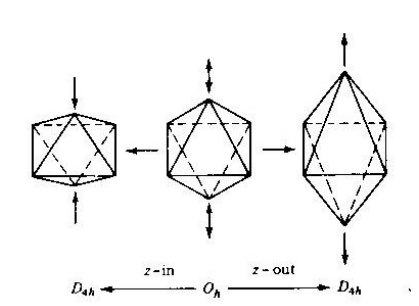


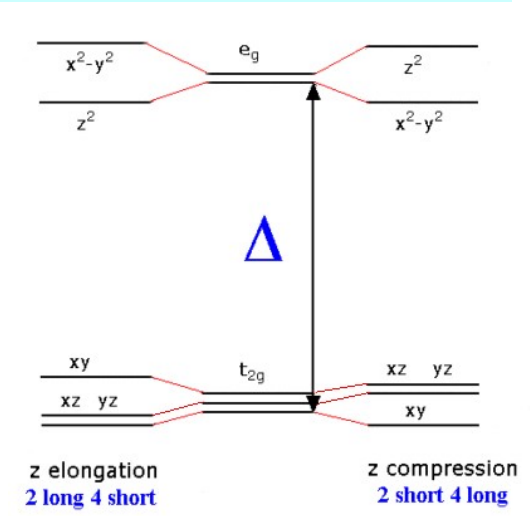
15

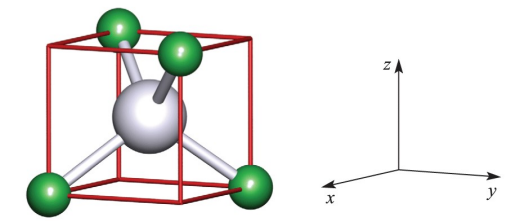
Jahn-Teller Distortions

The Jahn-Teller Theorem states: "any non-linear molecular system in a degenerate electronic state will be unstable and will undergo distortion to form a system of lower symmetry and lower energy thereby removing the degeneracy"

For octahedral coordination, susceptible species are d^4 , d^9 , and low spin d^7 in which 1 or 3 electrons occupy the e_q orbitals.

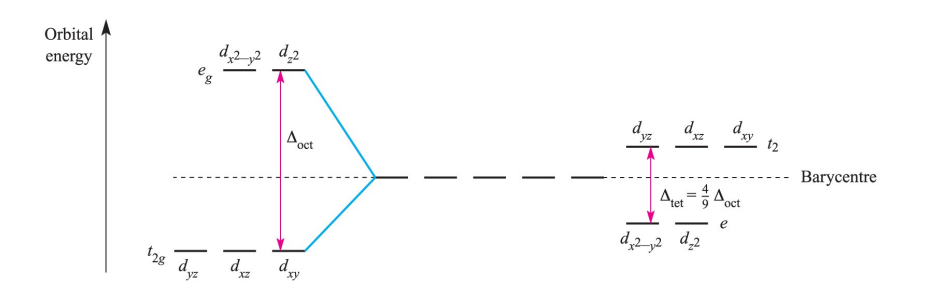




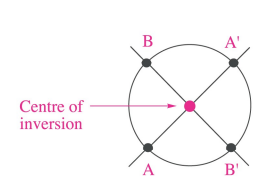


The relationship between a tetrahedral ML₄ complex and a cube; the cube is readily related to a Cartesian axis set.

Tetrahedral complexes are almost invariably high spin.



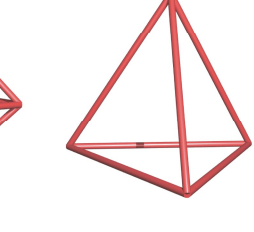
17



Point A is related to A' by passing through the centre of inversion. Similarly, B is related to B'.

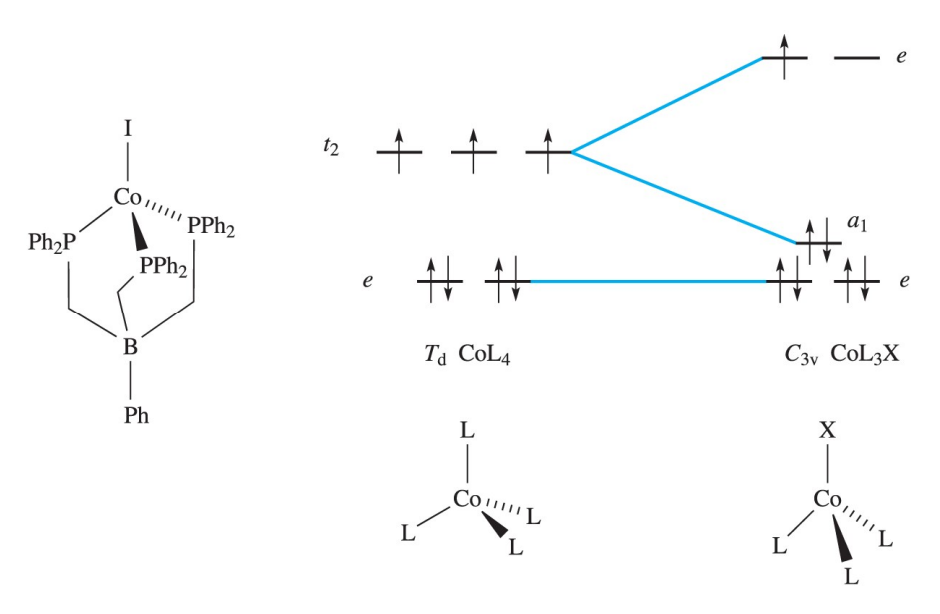


centre of symmetry

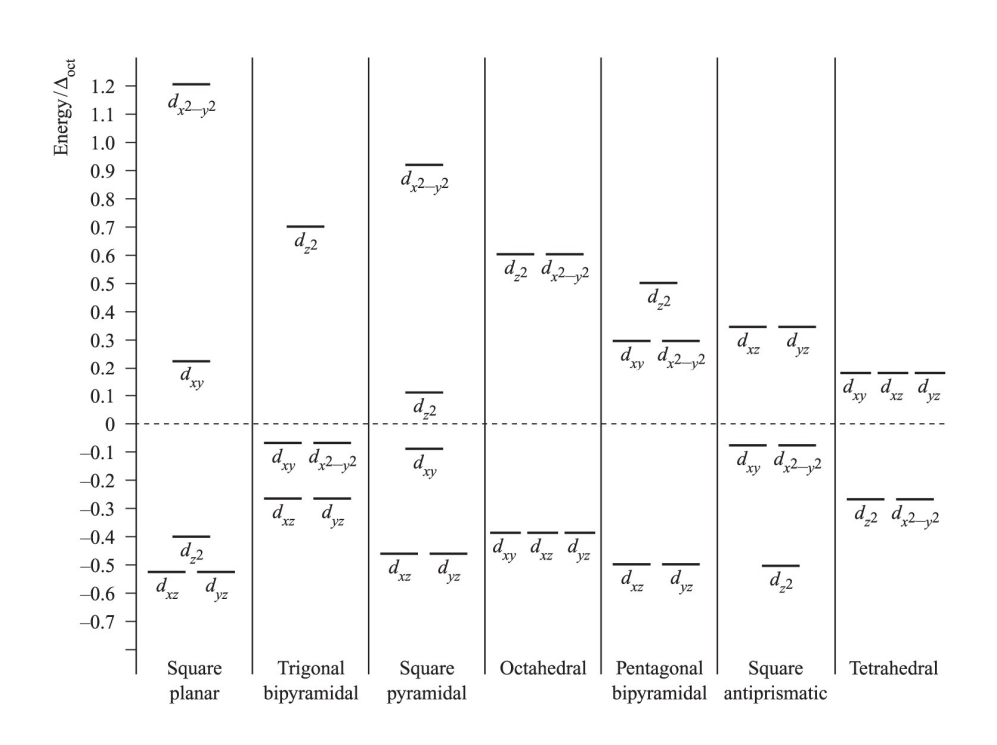


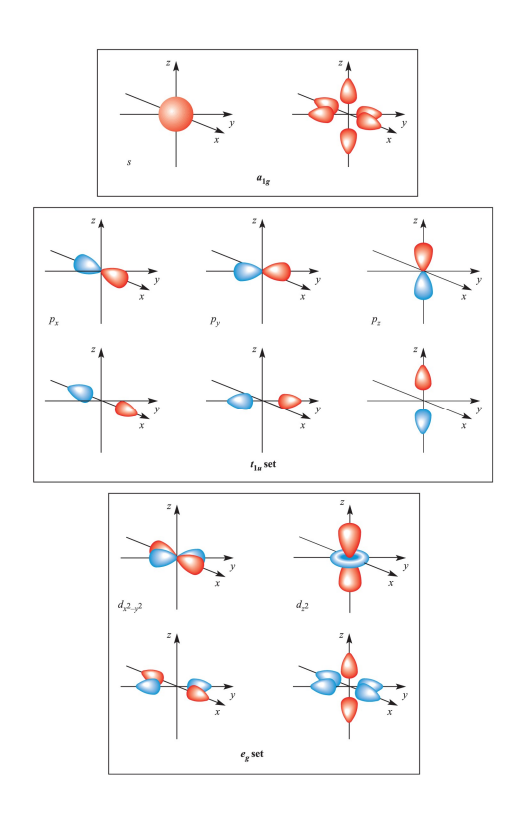
Tetrahedron: no centre of symmetry

Exception to the rule



Rare example of a low-spin, distorted tetrahedral complex

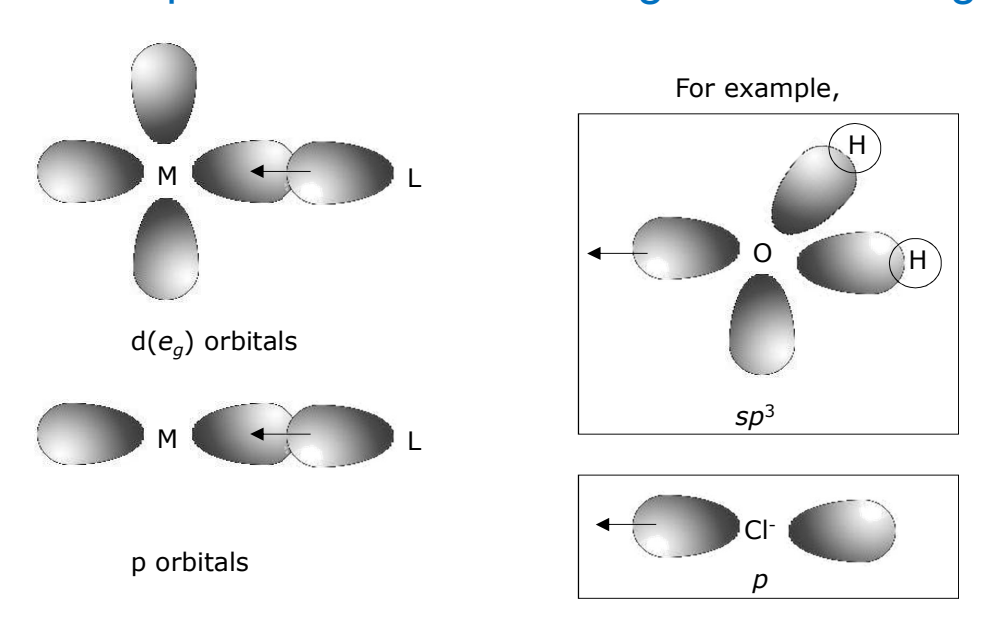




Complexes with no metalligand π bonding.

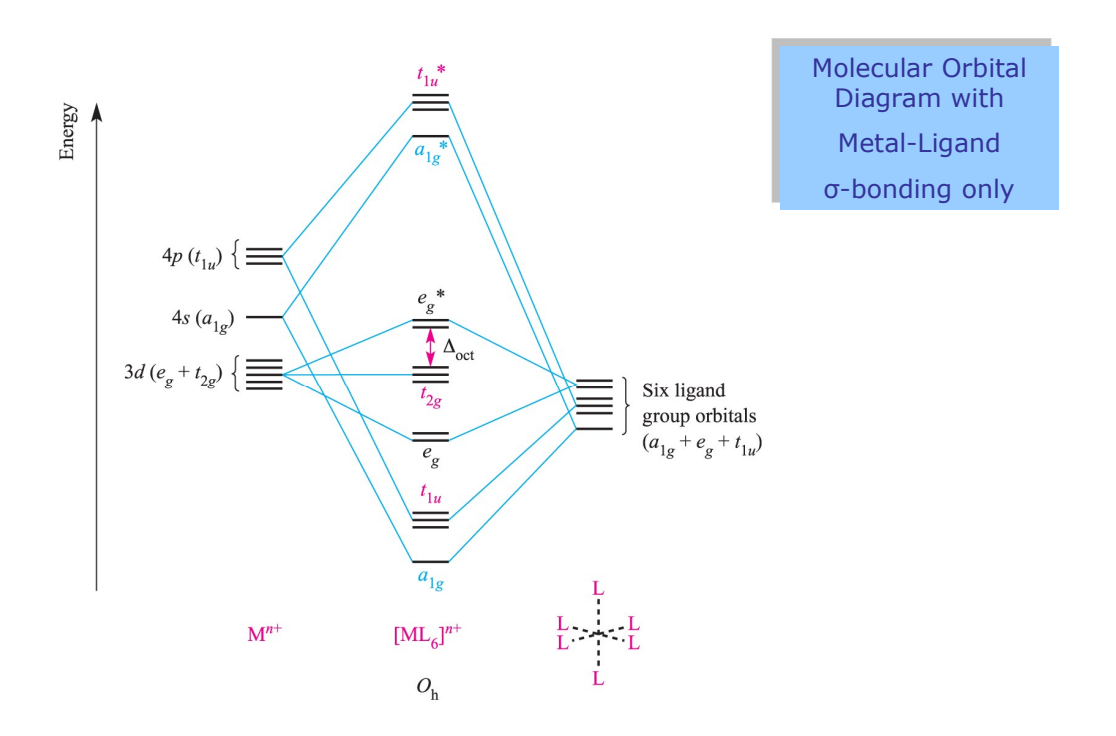
O _h (m3m)	Е	8C ₃	6C ₂	6C ₄	$3C_2 = C_4^2$	i	6S ₄	8 <i>S</i> ₆	$3\sigma_h$	6σ _d		
A _{1g}	1	1	1	1	1	1	1	1	1	1		$x^2 + y^2 + z^2$
A_{2g}	1	1	-1	-1	1	1	-1	1	1	-1		
E_g	2	-1	0	0	2	2	0	-1	2	0		$(2z^2 - x^2 - y^2,$ $\sqrt{3} (x^2 - y^2))$
T_{1g}	3	0	-1	1	-1	3	1	0	-1	-1	(R_x, R_y, R_z)	
T_{2g}	3	0	1	-1	-1	3	-1	0	-1	1		(xy, xz, yz)
A_{1u}	1	1	1	1	1	-1	-1	-1	-1	-1		
A_{2u}	1	1	-1	-1	1	-1	1	-1	-1	1		
E_u	2	-1	0	0	2	-2	0	1	-2	0		
T_{1u}	3	0	-1	1	-1	-3	-1	0	1	1	(x, y, z)	
T_{2u}	3	0	1	-1	-1	-3	1	0	1	-1		

Complexes with no metal-ligand π -bonding



 σ -type covalent interactions

23



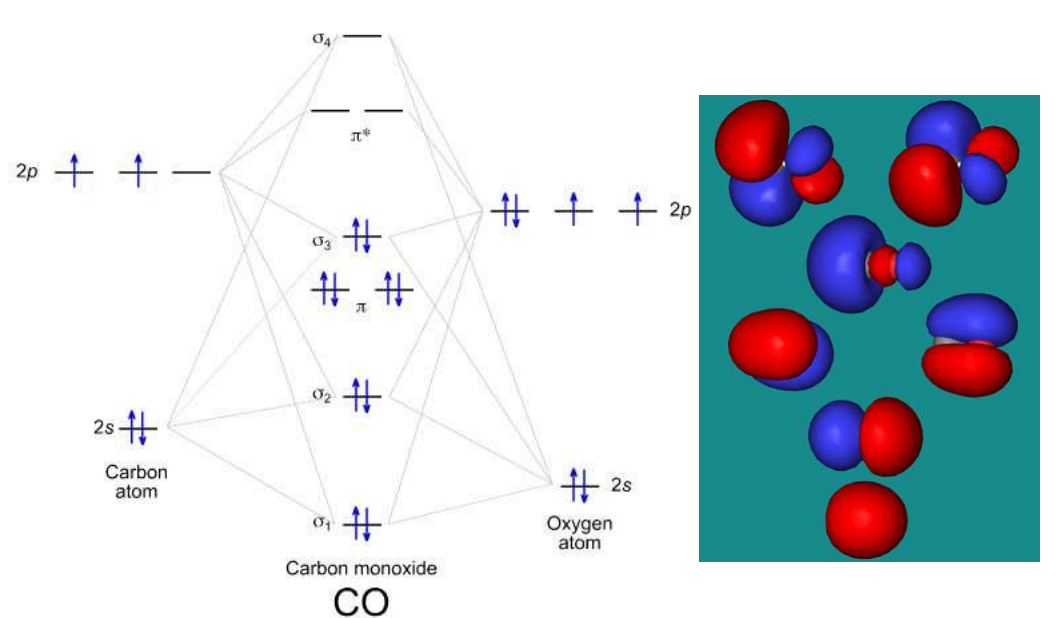
How many molecular orbitals are formed in an ML_6^{n+} complex with no metal-ligand π bonding?

How many of those molecular orbitals are bonding? ___ nonbonding? ___

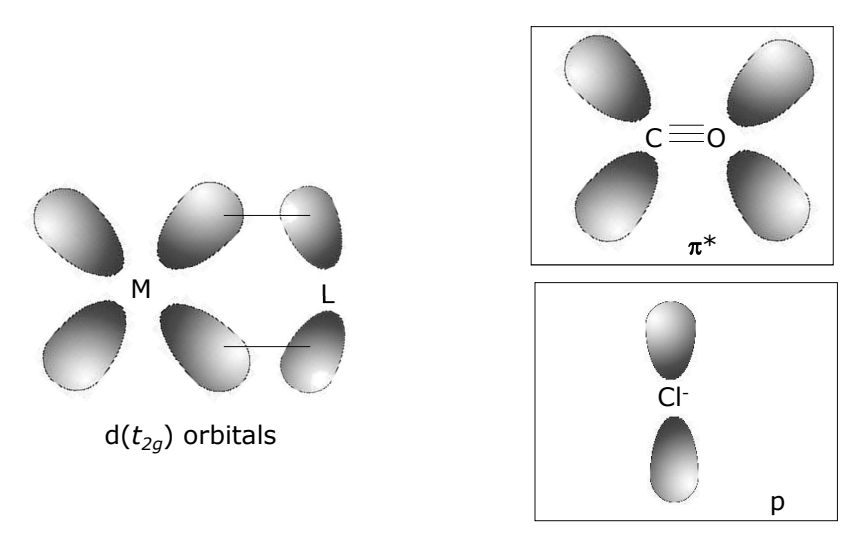
Sketch the orbital interactions for the bonding and antibonding molecular orbitals that arise from overlap between metal orbitals and ligand group orbitals in an ML_6^{n+} complex.

25

Complexes with metal-ligand π -bonding

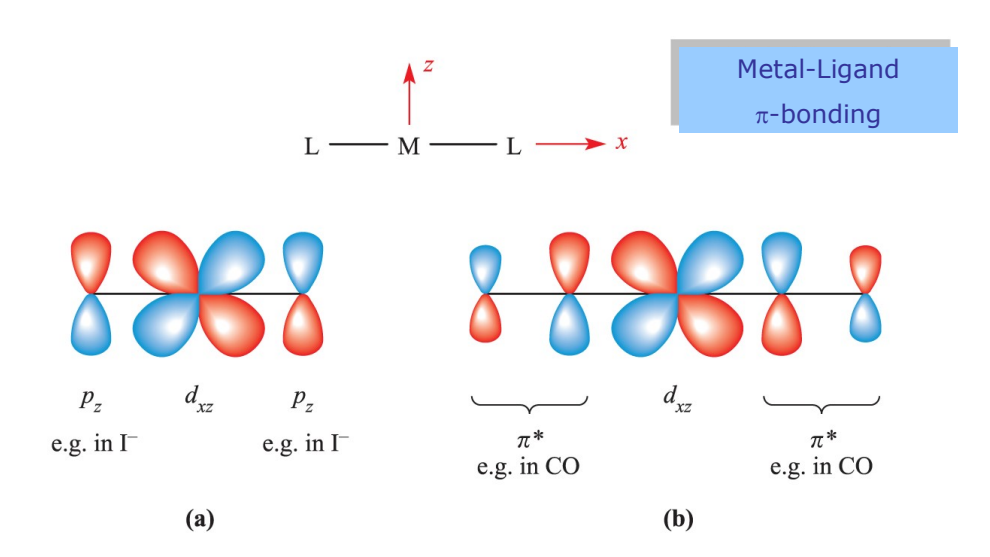


π -type covalent interaction



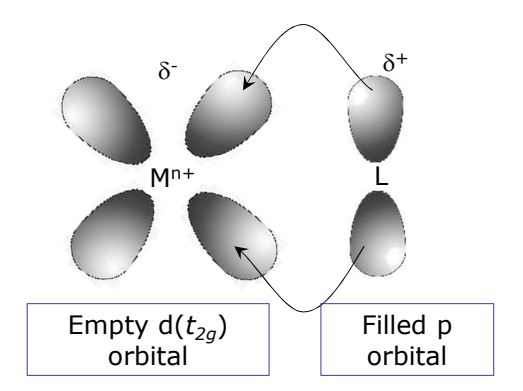
Can these π interactions explain some of the 'anomalies' in the spectrochemical series?

27



A π -donor ligand donates electrons to the metal center in an interaction that involves a filled ligand orbitals and an empty metal orbital.

A π -acceptor ligand accepts electrons from the metal center in an interaction that involves a filled metal orbitals and an empty ligand orbital.



Ligand-Metal π -bonding in a π -donor

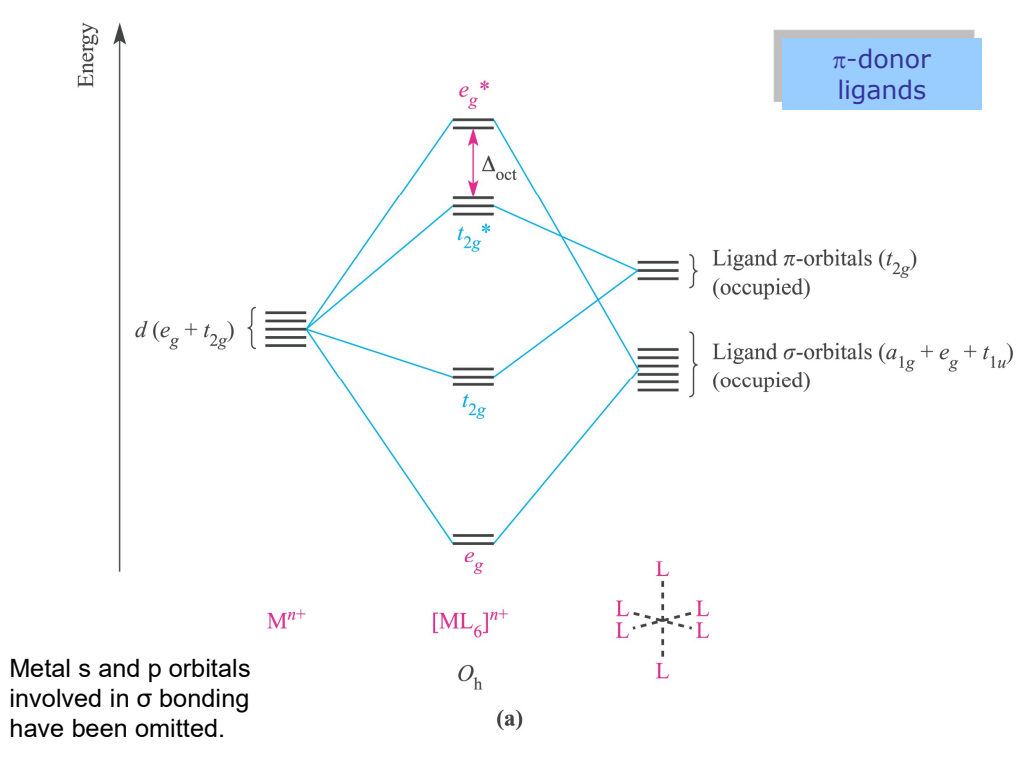
Yields a less polar M-L bond, resulting in diminished splitting.

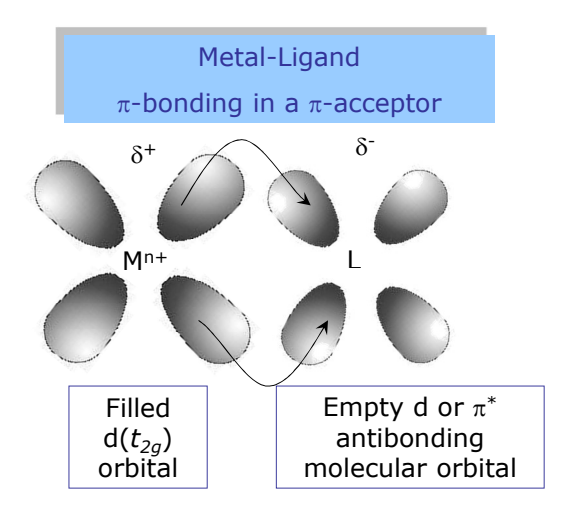
Typical ligands that exhibit this type of bonding include hydroxide (OH⁻), oxide (O²⁻), halides (I⁻, Br⁻, Cl⁻).

These ligands tend to be at the lower end of the spectrochemical series.

 $I^- < Br^- < S^{2^-} < Cl^- < {}^{S}CN^- < NO_3^- < N^{3^-} < F^- < OH^- < C_2O_4^{2^-} < H_2O < NCS^- < CH_3CN < py (pyridine) < NH_3 < en (ethylenediamine) < bipy (2,2'-bipyridine) < NO_2^- < PPh_3 < CN^- < CO$

29

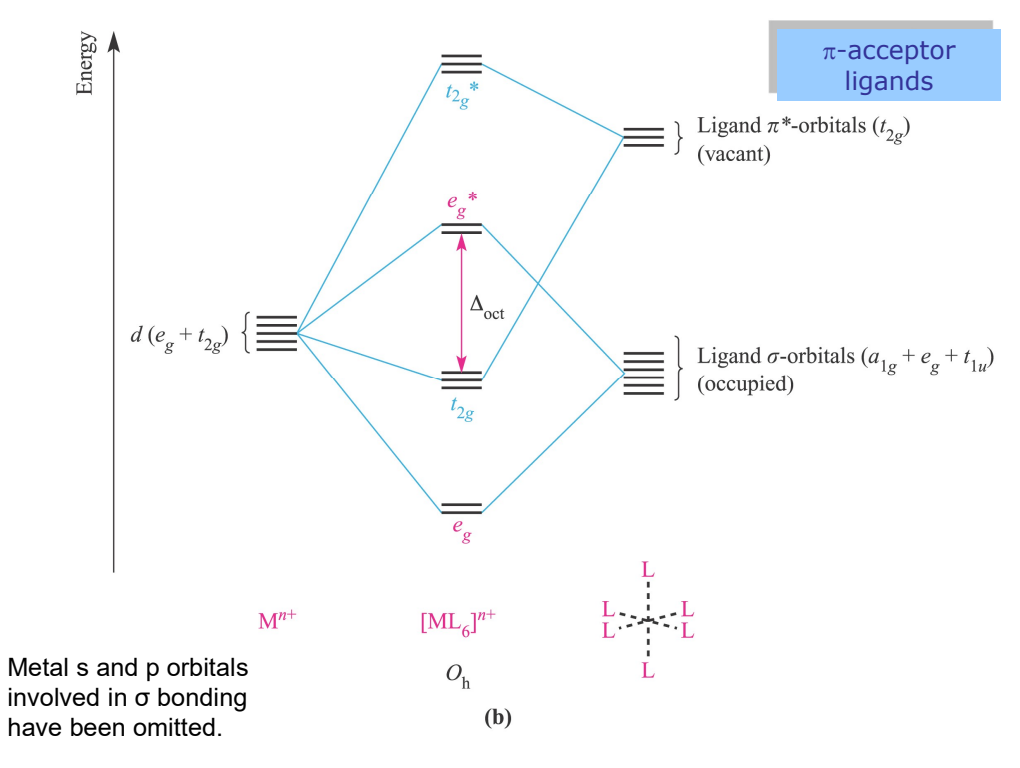




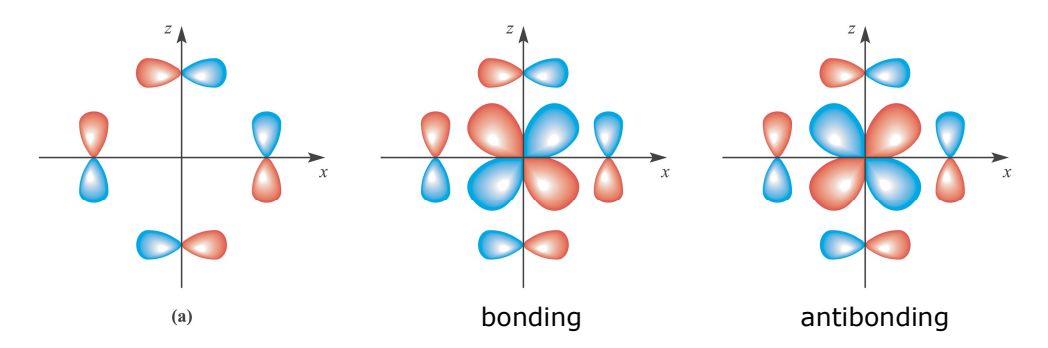
Backbonding between a filled metal orbital and an unfilled ligand orbital – has a greater polarity in the M-L bond and greater splitting of the d-orbitals.

Typical ligands that exhibit this type of bonding include phosphines (PR₃), arsines (AsR₃), cyanide (CN⁻), and carbonyl (CO).

31



Ligand Group π -orbitals



33

Describing electrons in multi-electron systems: L and M_L

Orbital angular momentum = $\left(\sqrt{l(l+1)}\right)\frac{h}{2\pi}$ $M_L = \sum m_l$ Orbital angular momentum has $\sqrt{6}(h/2\pi)$ $m_l = 2$ $+2(h/2\pi)$ magnitude and 2/+1 spatial orientations $\sqrt{6}(h/2\pi)$ $+(h/2\pi)$ with respect to the z $m_l = 1$ axis (i.e. the number of values of m_I), $m_l = 0$ 0 $\sqrt{6}(h/2\pi)$ vectorial summation of the individual I values is necessary $m_1 = -1$ $-(h/2\pi)$ $\sqrt{6}(h/2\pi)$ (review Box 1.5). $m_1 = -2$ $-2(h/2\pi)$ $\sqrt{6}(h/2\pi)$ Orbital angular momentum = $\left(\sqrt{L(L+1)}\right)\frac{h}{2\pi}$

Describing electrons in multi-electron systems: S and M_S

The spin quantum number, s, determines the magnitude of the spin angular momentum of an electron and has a value of $\frac{1}{2}$.

For a 1 electron species, m_s is the magnetic spin angular momentum and has a value of $\pm \frac{1}{2}$ or $\pm \frac{1}{2}$.

S is the total spin quantum number

Spin angular momentum = $\left(\sqrt{S(S+1)}\right)\frac{h}{2\pi}$ for a multi-electron system

$$M_S = \sum m_s$$

For a system with n electrons, each having $s = \frac{1}{2}$, possible values of S (always positive) fall into two series depending on the total number of electrons:

•S = 1/2, 3/2, 5/2, for an odd number of electrons.

•S = $0, 1, 2, \dots$ for an even number of electrons.

For each value of S, there are (2S + 1) values of M_S :

$$M_{S}$$
: S, (S-1), ...-(S-1), -S

35

Microstates and term symbols

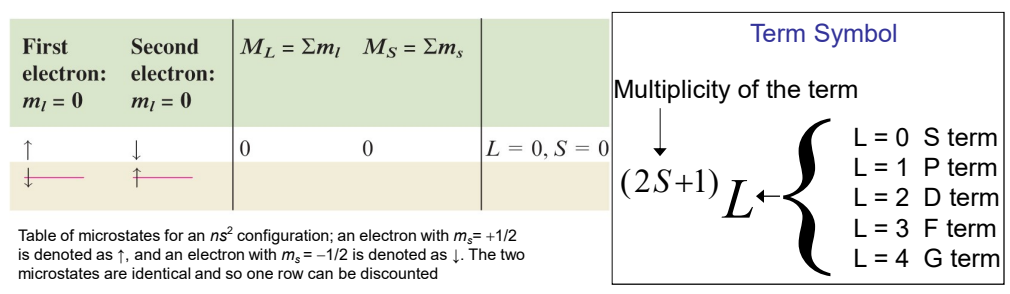
Microstates – the electronic states that are possible for a given electronic configuration.

- •no two electrons may have the same set of quantum numbers (Pauli exclusion principle)
- only unique microstates may be included

ns2 configuration

Cannot physically distinguish between the electrons, so must use sets of quantum numbers to decide if the microstates (rows in the table) are the same or different.

First microstate:
$$I = 0$$
, $m_I = 0$, $m_S = +1/2$; $I = 0$, $m_I = 0$, $m_S = -1/2$
Second microstate: $I = 0$, $m_I = 0$, $m_S = -1/2$; $I = 0$, $m_I = 0$, $m_S = +1/2$



Terms for which (2S+1) = 1,2,3,4,... are called singlet, doublet, triplet, quartet

ns¹ n's¹ configuration

First electron: $m_l = 0$	electron:	$M_L = \sum m_l$	$M_S = \sum m_s$	
\uparrow	\uparrow	0	+1)
↑	\	0	0	L = 0,
\downarrow	\	0	-1	$\int S = 1$

Table of microstates for an $ns^1n's^1$ configuration. An electron with $m_s = +1/2$ is denoted as \uparrow , and an electron with $m_s = -1/2$ as \downarrow . Each row in the table corresponds to a different microstate.

37

Describing electrons in multi-electron systems: J and M_1

Total angular momentum =
$$\left(\sqrt{J(J+1)}\right)\frac{h}{2\pi}$$

Total angular momentum quantum number J takes values: (L + S), (L + S - 1) ... |L-S| and these values can be 0, 1, 2 ... or 1/2, 3/2, 5/2, ...

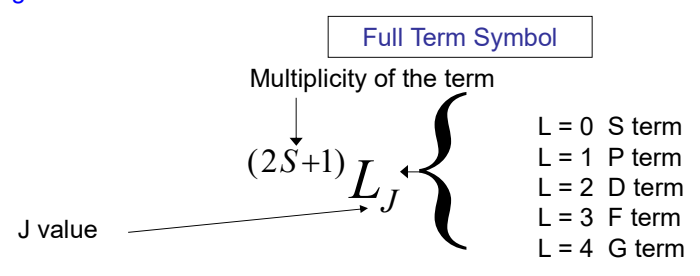
Case 1: (2S + 1) possible values of J for S < L

Case 2: (2L + 1) possible values of J for L < S.

The value of M_J denotes the component of the total angular momentum along the z axis.

Allowed values of M_J : J, J-1, ..., -(J-1), -J.

The method of obtaining J from L and S is based on LS (or Russell –Saunders) coupling, aka spin-orbit coupling.



Rules for Constructing a table of microstates

- 1. Write down the electron configuration (e.g. d²)
- 2. Ignore closed shell electron configurations (e.g. ns^2 , np^6 , nd^{10}) as these will always give a 1S_0 term.
- 3. Determine the number of microstates: for x electrons in a sublevel of (2I+1) orbitals, this is given by:

$$\frac{\{2(2l+1)\}!}{x!\{2(2l+1)-x\}!}$$

- 4. Tabulate microstates by m_l and m_s , and sum to give M_L and M_S on each row. Check that the number of microstates in the table is the same as that expected from rule 3.
- 5. Collect the microstates into groups based on values of M_L .

39

Microstates for Hydrogen, Z = 1.

Number of microstates =
$$\frac{\{2(2l+1)\}!}{x!\{2(2l+1)-x\}!} = \frac{2!}{1!*1!} = 2$$

$m_l = 0$	$M_L = \Sigma m_I$	$M_{S} = \Sigma m_{S}$	
↑	0	+1/2	า
	0	-1/2	L = 0, S = 1/2

$${}^{2}S_{1/2}$$

Microstates for Helium, Z = 2.

Lithium, Z = 3.

 ${}^{2}S_{1/2}$

Beryllium, Z = 4.

 ${}^{1}S_{0}$

41

Microstates for Boron, Z = 5.

Only the 2p¹ configuration contributes, but there are 3 distinct p orbitals.

Number of microstates =
$$\frac{\{2(2l+1)\}!}{x!\{2(2l+1)-x\}!} = \frac{6!}{1! \times 5!} = 6$$

$m_l = +1 \ m_l = 0 \ m_l = -1$	$M_L =$	M _S =	
	Σm_l	$\Sigma m_{ m S}$	
\uparrow	+1	+1/2	
↑	0	+1/2	\
↑	-1	+1/2	$\int L = 1, S = 1/2$
\	-1	-1/2	
\	0	-1/2	\
\	+1	-1/2	S L = 1, S = 1/2

$${}^2P_{3/2}$$
 or ${}^2P_{1/2}$

Hund's Rules

Providing that Russell-Saunders coupling holds:

For the relative energies of terms for a given electronic configuration:

- 1. The term with the highest spin multiplicity has the lowest energy.
- 2. If two or more term have the same multiplicity (e.g. 3F and 3P), the term with the highest value of L has the lowest energy (e.g. 3F is lower than 3P)
- 3. For terms having the same multiplicity and the same values of L (e.g. 3P_0 and 3P_1):
- The level with the lowest value of *J* is the lowest in energy if the sub-level is less than half-filled (e.g. p²).
- The level with the highest value of *J* is more stable if the sub-level is more stable if the sub-level is more than half filled (e.g. p⁴).
- The level is half-filled with maximum spin multiplicity (e.g. p³ with S = 3/2), L must be zero, and J = S.

43

$m_l = +1$	$m_l = 0$	$m_l = -1$	M_L	M_S		
$\uparrow\downarrow$			2	0)	
↑	\downarrow		1	0		
	$\uparrow\downarrow$		0	0	L = 2, S = 0	
	\uparrow	\downarrow	-1	0		
		$\uparrow\downarrow$	-2	0)	
↑	\uparrow		1	1		
1		\uparrow	0	1		
	\uparrow	↑	-1	1		
\downarrow	\uparrow		1	0		
\downarrow		↑	0	0	L = 1, S = 1	
	\downarrow	1	-1	0		
\downarrow	\downarrow		1	-1		
1		\downarrow	77.00	-1		
	\downarrow	\downarrow	-1		\	
\uparrow		\downarrow	0	0	$\bigg\}\ L=0,S=0$	

Number of microstates = $\frac{\{2(2l+1)\}!}{x!\{2(2l+1)-x\}!} = \frac{6!}{2! \times 4!} = 15$

Microstates for Carbon, Z = 6.

 $2s^22p^2$

Microstates for d^2

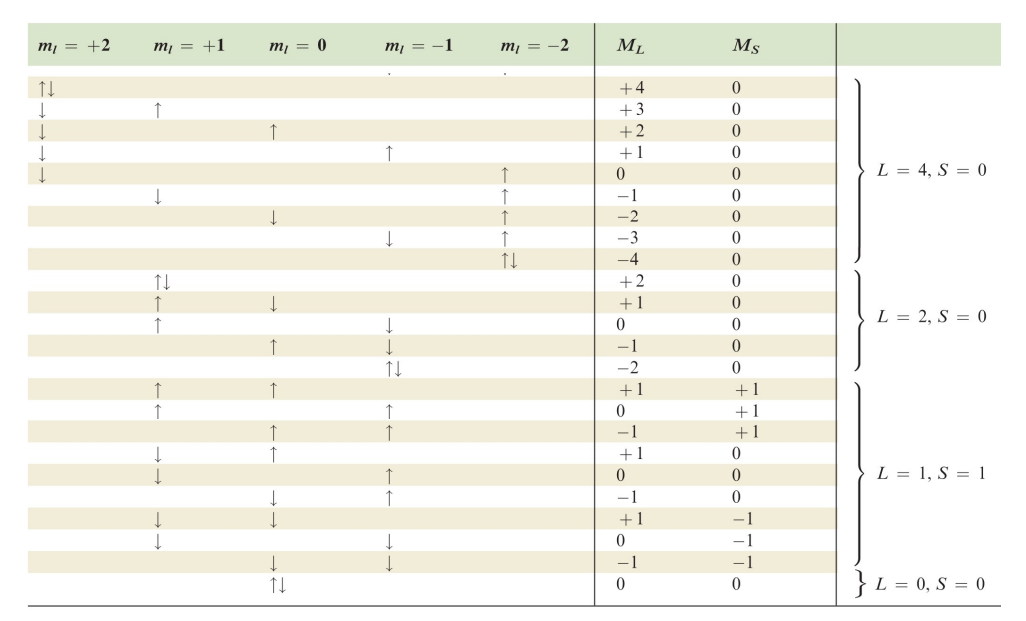
Number of microstates =
$$\frac{\{2(2l+1)\}!}{x!\{2(2l+1)-x\}!} = \frac{10!}{2! \times 8!} = 45$$

$m_l = +2$	$m_l = +1$	$m_l = 0$	$m_l = -1$	$m_l = -2$	M_L	M_S	
1	1				+ 3	+ 1)
1		1			+2	+1	
1			↑		+1	+1	
1				1	0	+1	
	1			↑	-1	+1	
		1		1	-2	+1	
			1	1	-3	+1	
1	\downarrow				+3	0	
1		1			+2	0	
1			\downarrow		+1	0	
1				1	0	0	L = 3, S = 1
	1			↓	-1	0	
		1		1	-2	0	
			1	↓	-3	0	
1	1				+3	-1	
1		1			+2	-1	
1			<u></u>		+1	-1	
1				1	0		
	1			1	-1	-1	
		1		1	-2	-1	
			↓	↓	-3	-1	,

Term symbols:

45

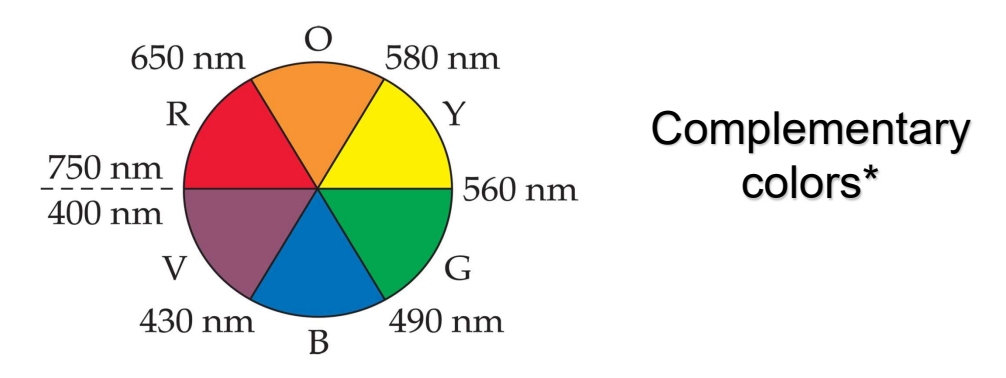
Microstates for d², cont.



Energy ordering of terms using Hund's Rules:

Complexes and color

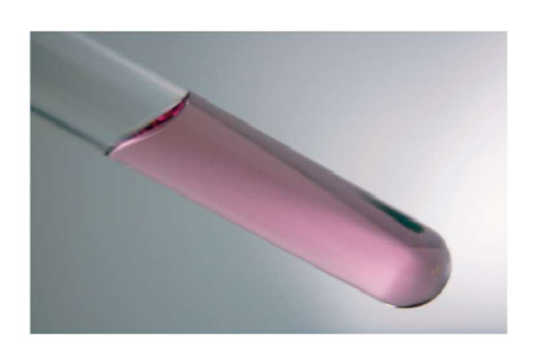
- •A substance appears black if it absorbs all the visible light that strikes it, whereas if a substance absorbs no visible light it is white or colorless.
- •An object appears green if it *reflects* all colors except red, the complementary color of green.
- •Similarly, this concept applies to transmitted light that pass through a solution.



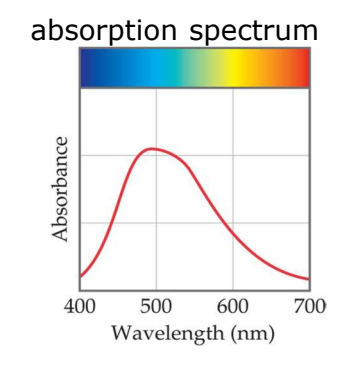
*Assuming a simple absorption

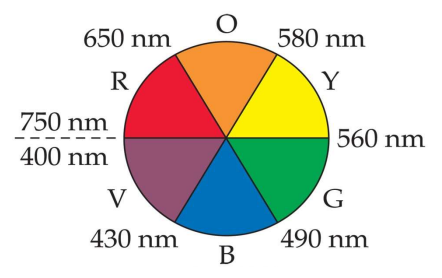
47

Complexes and color



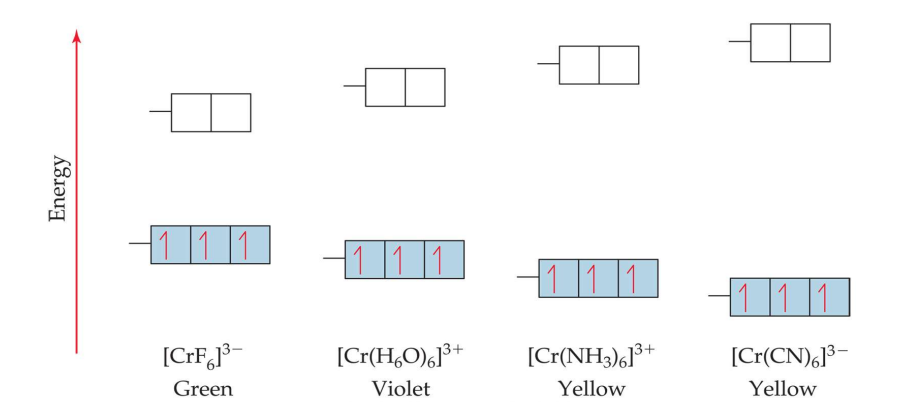
 $[Ti(H_2O)_6]^{3+}$ appears red-violet in color because it absorbs light at the center (yellow and green) parts of the spectrum.





Complexes and color

Interactions between electrons on a ligand and the orbitals on the metal cause differences in energies between orbitals in the complex. (*d-d* transitions)



49

Charge-transfer transitions KMnO₄ K₂CrO₄ KCIO₄ Empty Mn 3d orbitals Absorbance 0.8 t_2 set $\lambda_{\text{max}} = 528 \, \text{nm}$ Energy 2.0 e set 1.0 0.0 270 350 430 510 590 670 750

50

Filled ligand orbitals

Wavelength (nm)

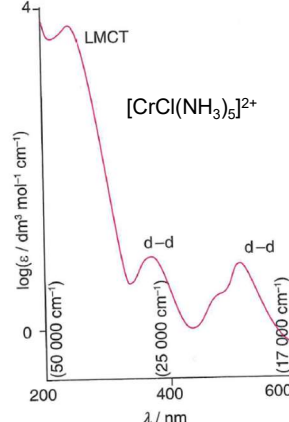
Two types of charge transfer absorptions

- 1.Transfer of an electron from an orbital with primarily ligand character to one with primarily metal character (*ligand to metal charge transfer*, **LMCT**)
- 2.Transfer of an electron from an orbital with primarily metal character to one with primarily ligand character (*metal-to-ligand charge transfer*, **MLCT**)

Electron transfer in LMCT occurs when a ligand that is easily oxidized is bound to a metal center that is readily reduced.

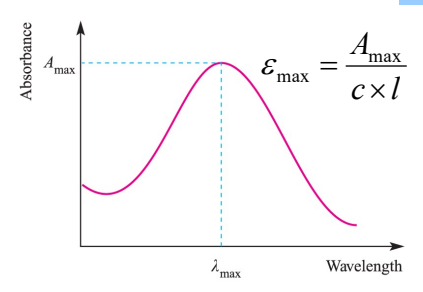
Electron transfer in MLCT occurs when a ligand that is easily reduced is bound to a metal center that is readily oxidized.

Probability of these electronic transitions is <u>high</u>, therefore the absorption bands are intense.



51

Electronic Spectra



Absorption bands are usually broad, as a consequence of the <u>Franck-Condon</u> <u>Approximation</u>, which states that electronic transitions are very much faster than nuclear motion (nuclear mass is far greater than electron mass).

Absorption bands are described in terms of λ_{max} (nm or cm⁻¹) and absorption maximum.

Type of transition	Typical $\varepsilon_{\rm max}/{\rm dm}^3~{\rm mol}^{-1}~{\rm cm}^{-1}$	Example
Spin-forbidden 'd-d'	<1	$[Mn(OH_2)_6]^{2+}$ (high-spin d^5)
Laporte-forbidden, spin-allowed 'd-d'	1–10 10–1000	Centrosymmetric complexes, e.g. $[\text{Ti}(OH_2)_6]^{3+}$ (d^1) Non-centrosymmetric complexes, e.g. $[\text{NiCl}_4]^{2-}$
Charge transfer (fully allowed)	1000-50 000	$[\mathrm{MnO_4}]^-$

- •d¹, d⁴, d⁶, and d⁹ complexes consist of one broad absorption.
- •d², d³, d⁷, and d⁸ complexes consist of three broad absorption.
- •d⁵ complexes consist of a series of very weak, relatively sharp absorptions. (instrument, solvent, and cuvette limitations)

Selection Rules

The strength of an electronic transition is determined by the transition dipole moment

Spin selection rule: $\Delta S = 0$

-Transitions may occur from singlet to singlet, or from triplet to triplet states etc., but a change in *spin multiplicity* is *forbidden* and are generally weaker than spin allowed transitions.

Laporte selection rule: in a centrosymmetric molecule or ion, the only allowed transitions are those accompanied by a change in *parity*:

allowed transitions: $g \leftrightarrow u$

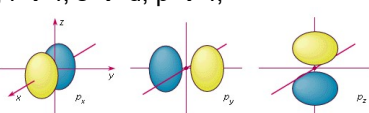
forbidden transitions: $g \leftrightarrow g$, $u \leftrightarrow u$

This leads to the selection rule:

 $\Delta I = \pm 1$

allowed transitions are: $s \rightarrow p$, $p \rightarrow d$, $d \rightarrow f$,

forbidden transitions are: $s \rightarrow s$, $p \rightarrow p$, $d \rightarrow d$, $f \rightarrow f$, $s \rightarrow d$, $p \rightarrow f$,

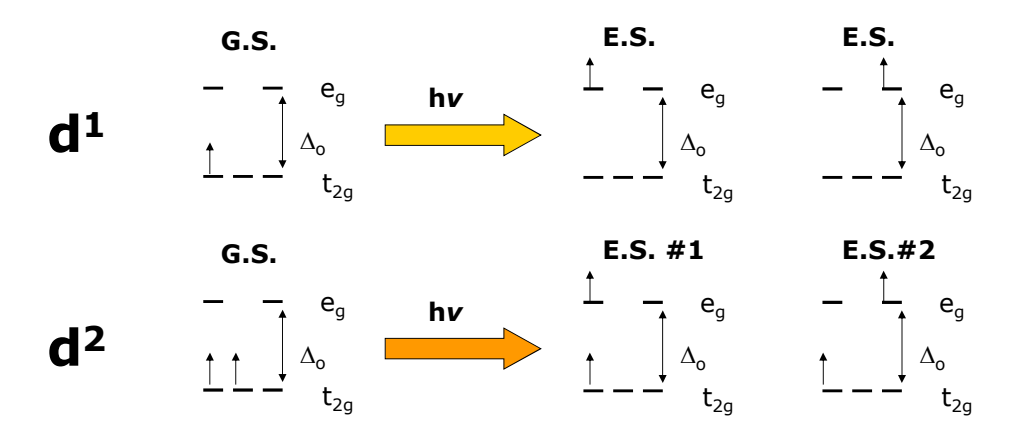


53

dⁿ Transitions

We must remember that any $\mathbf{d} \Rightarrow \mathbf{d}$ transitions observed are "spin-allowed".

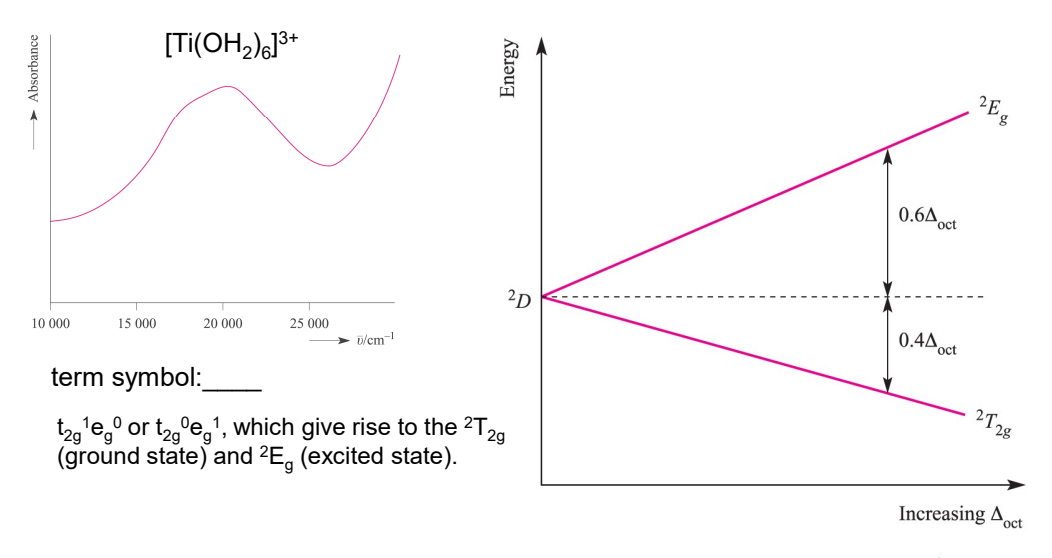
This means that in such a d^n configuration you will observe as many excited states (E.S.) as is possible as long as the spin of the electron doesn't change.



Splitting of Terms

Term	Components in an octahedral field
S	A_{1g}
Р	T_{1g}
D	$T_{2g} + E_{g}$
F	$A_{2g} + T_{2g} + T_{1g}$
G	$A_{1g} + E_{g} + T_{2g} + T_{1g}$
Н	$E_{g} + T_{1g} + T_{1g} + T_{2g}$
I	$A_{1g} + A_{2g} + E_g + T_{1g} + T_{2g} + T_{2g}$
(Lantha	anide metal ions have ground state H and I terms)

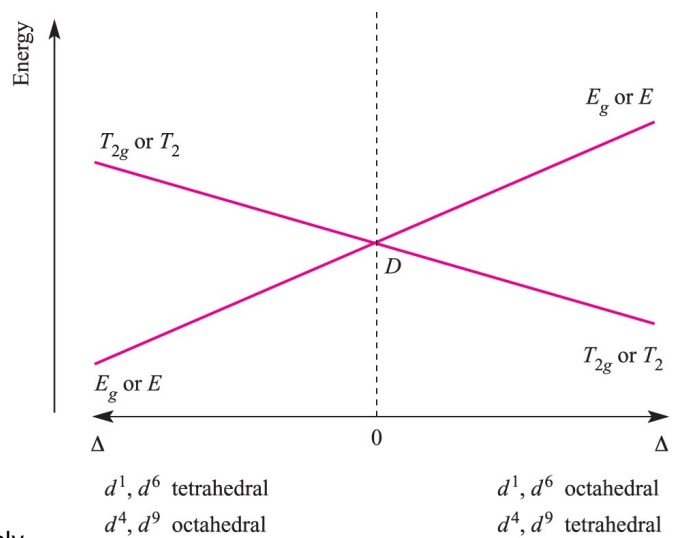
55



Energy level diagram for a d^1 ion in an octahedral field.

Orgel Diagram

Correlation between free atom terms and terms of a complex can be displayed on an Orgel diagram.

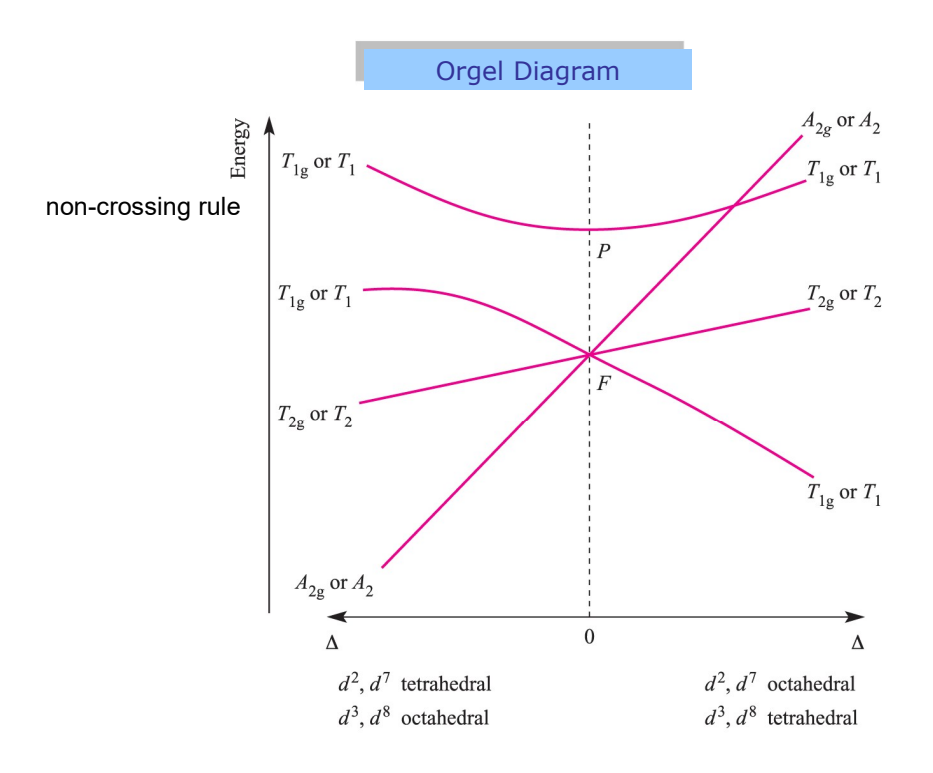


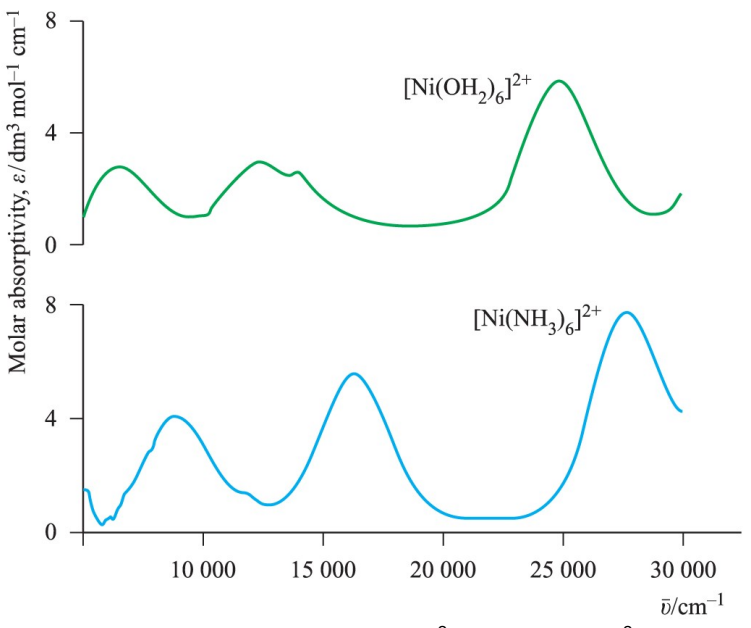
High spin only

57

microstates: d²

Consider if a splitting of the terms would occur in an octahedral or tetrahedral fields.





Electronic spectra of $[\mathrm{Ni}(\mathrm{OH_2})_6]^{2^+}$ and $[\mathrm{Ni}(\mathrm{NH_3})_6]^{2^+}$

Consider a maximum absorption at 520 nm...

$$v = c/\lambda = (3.00 \times 10^8 \text{ m/s})/(520 \times 10^{-9} \text{ m})$$

= 5.77 x 10¹⁴ s⁻¹

Often, the number used by spectroscopists is the wavenumber (reciprocal of the wavelength in cm)

$$\overline{v}$$
 (cm⁻¹)= 1/ λ = 1/[(520 x 10⁻⁹ m)(100 cm/m)] = 19200 cm⁻¹

For octahedral d^1 systems, one can directly correlate the absorption with the value Δ_{o}

 $\Delta_0 = (hc/\lambda)N$

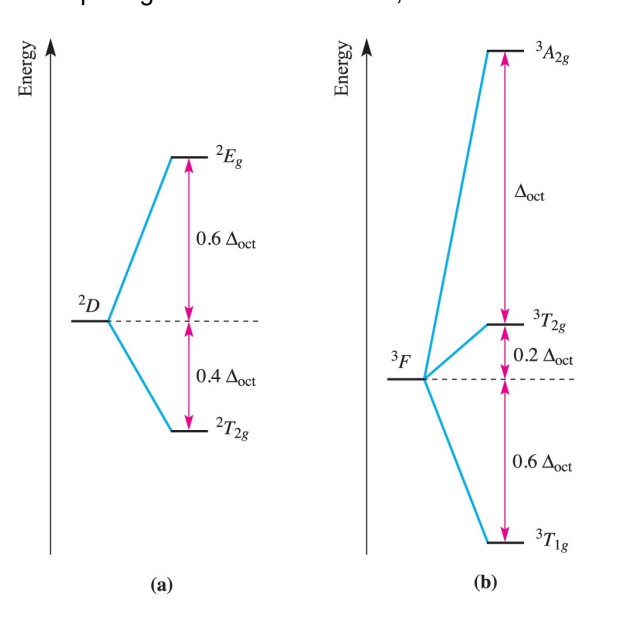
= $[(6.626 \times 10^{-34} \text{ Js})(3.00 \times 10^8 \text{ m/s})/520 \times 10^{-9} \text{ m}] \times (6.022 \times 10^{23} /\text{mol})$

= 230 kJ/mol

Reminder: in general, the absorptions are more complex and have to do with the orbital and spin electronic motions (coupling).

61

Splitting in an octahedral field, weak field limit



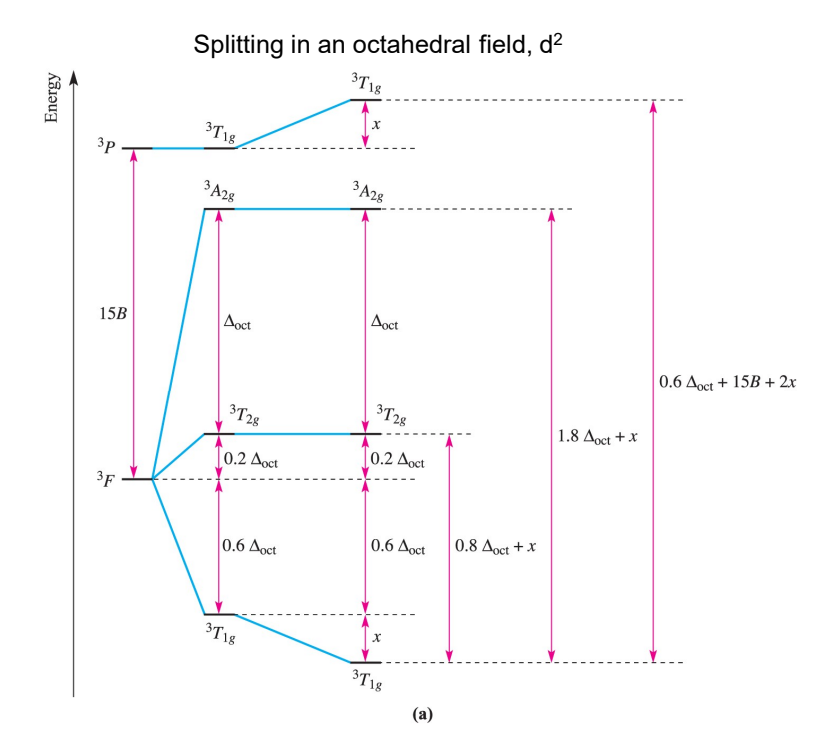
²D term arising from a d¹ configuration

³F term arising from a *q*² configuration

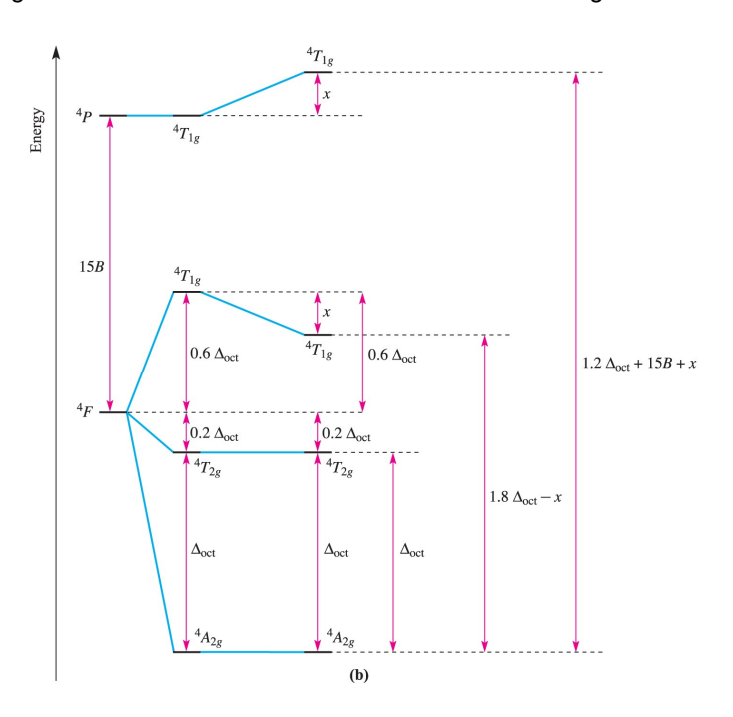
Racah parameters (A, B, C)

- Summarize the effects of electron-electron repulsion on the energies of the terms that arise from a single configuration.
- Parameters are a quantitative expression of ideas underlying Hund's rules and account for deviations from them.
- Empirical quantities obtained from gas phase atomic spectroscopy.

Example: Ti^{2+} (d^2) $B = 720 \text{ cm}^{-1}$ C/B = 3.7

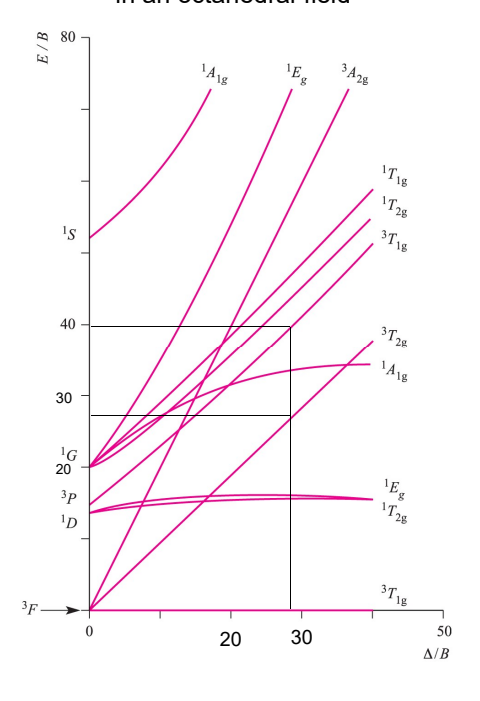


Splitting in an octahedral field of the 4F and 4P terms arising from a d^3

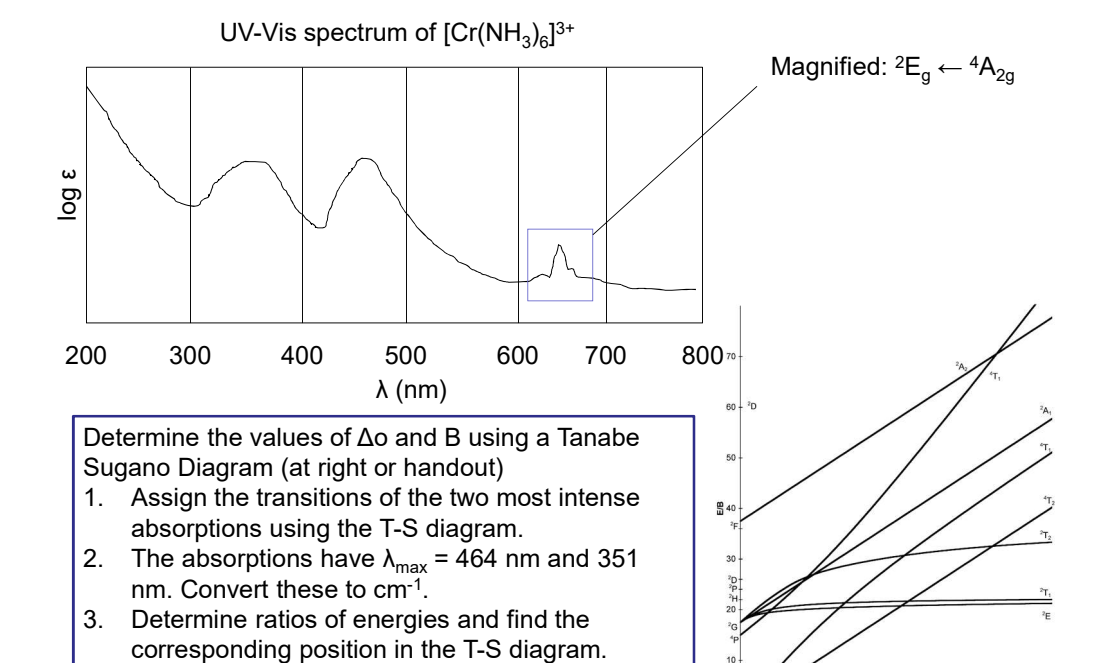


Tanabe-Sugano

Diagram for a d² ion in an octahedral field



65



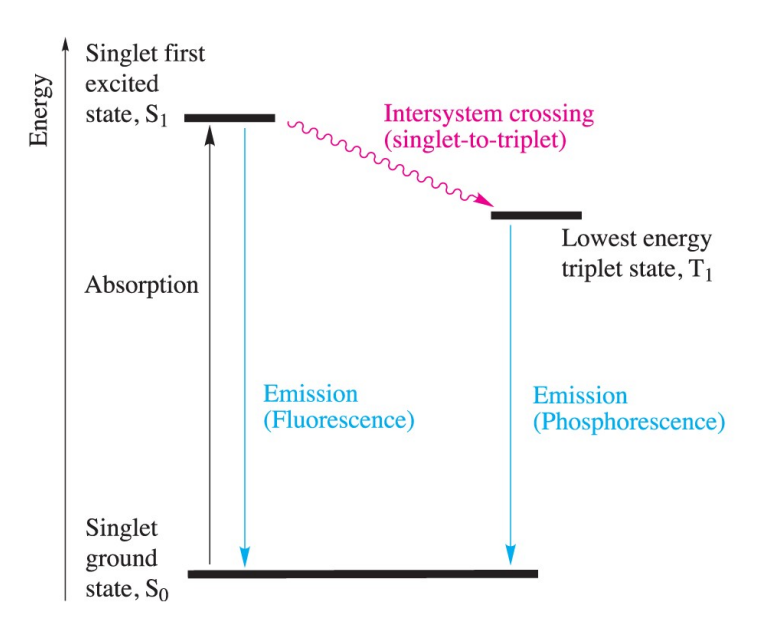
66

4. Determine the value of B 5. Determine the value of Δ_0

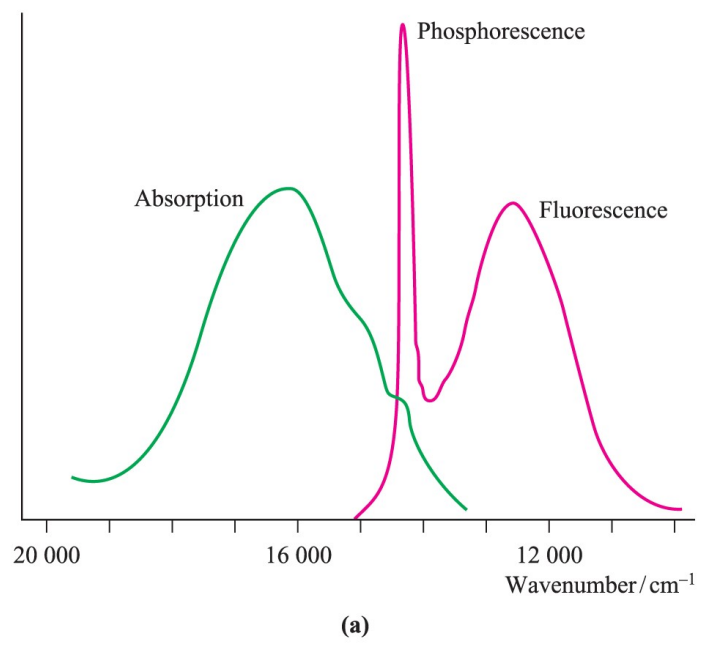
Ligand substitution reactions are used to prepare different complexes, for example one could prepare $[Cr(H_2O)_6]^{3+}$ from $[Cr(NH_3)_6]^{3+}$. In consideration of the ligand field strength of H_2O compared to NH_3 , do you expect a shift to higher or lower wavelength for the absorptions?

Use the d³ Tanabe-Sugano diagram to predict the energies of the first two spin-allowed quartet bands in the spectrum of $[Cr(H_2O)_6]^{3+}$ for which Δ_o = 17,600 cm⁻¹ and B = 700 cm⁻¹. Sketch the expected UV-Vis spectrum, labeling both the x-axis (nm) and y-axis (ϵ). Provide a justification for magnitude of values on the y-axis.

67



Emission processes are represented using a Jablonski diagram. Radiative and non-radiative transitions are depicted by straight and wavy arrows, respectively.



In a fluorescence experiment, an absorption spectrum is collected.

A sample is then irradiated with light corresponding to wavelength of maximum absorbance, and the emission spectrum is recorded.

The absorption (at 298 K) and emission (at 77 K) spectra of [Cr{OC(NH₂)₂}₆]³⁺

69

Nephelauxetic effect

(electron) 'cloud expanding'

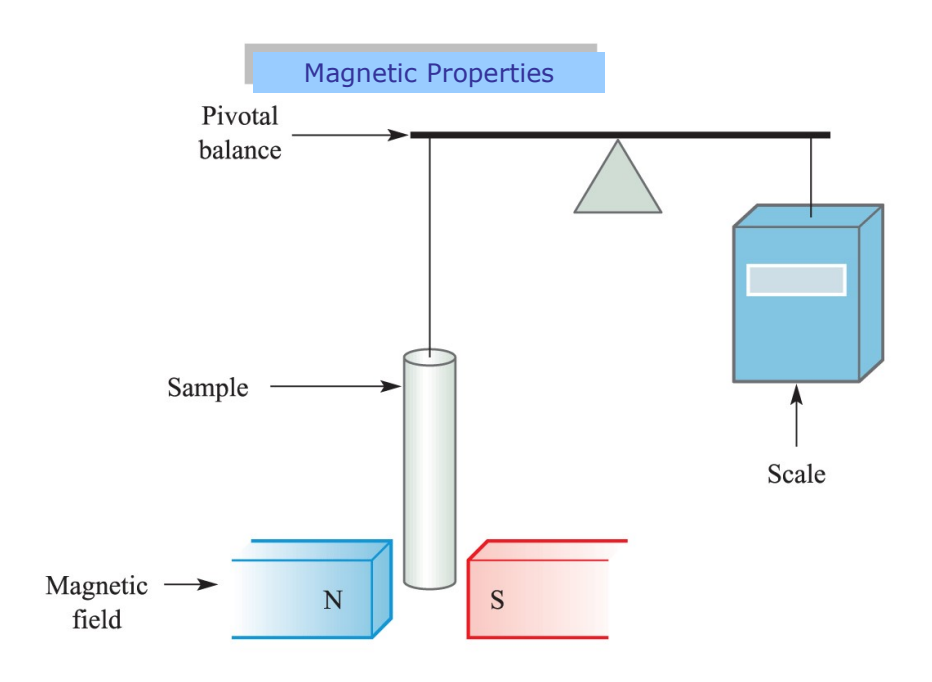
Pairing energies are <u>lower</u> in complexes than in gaseous metal ions, indicating that *interelectronic repulsion is less* in complexes and that the effective size of the metal orbitals has increased, which is known as the **nephelauxetic effect**.

Metal ion	k	Ligands	h
Co(III)	0.35	$6~\mathrm{Br}^-$	2.3
Rh(III)	0.28	6 Cl ⁻	2.0
Co(II)	0.24	6 [CN] ⁻	2.0
Fe(III)	0.24	3 en	1.5
Cr(III)	0.21	6 NH ₃	1.4
Ni(II)	0.12	6 H ₂ O	1.0
Mn(II)	0.07	$6~\mathrm{F}^-$	0.8

Adjusts the Racah parameter B

 $(B_0 - B)/B_0 \approx h_{ligands} \times k_{metal ion}$

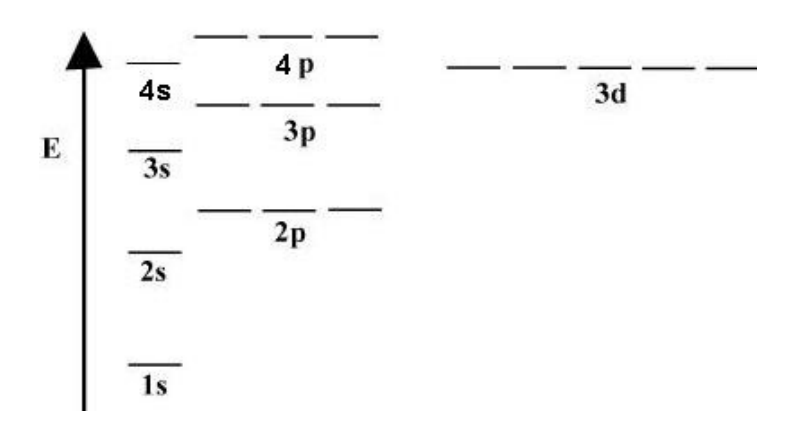
Selected values of h and k which are used to parameterize the nephelauxetic series



Schematic representation of a Gouy balance.

71

Magnetic Properties



Relative orbital energies of a typical first-row transition metal.

- •Note that each $n \ge 2$ orbitals are no longer degenerate (in non-H atom).
- •Energy increases with / value.



<u>Diamagnetism</u> – results in a compound being repelled by a magnetic field.



Water and other compounds with paired electrons exhibit diamagnetism.

<u>Paramagnetism</u> – a property of compounds with one or more unpaired electrons that results in a compound being drawn into a magnetic field.

Paramagnetism is much stronger than diamagnetism, and a *paramagnetic* substance that is drawn into the field appears to weigh *more* in the presence of a magnetic field, whereas *diamagnetic* substances appear to weigh slightly *less* in the presence of a magnetic field.

<u>Molar susceptibility</u> – is a macroscopic property of compounds that reflects a magnetic moment, μ , a microscopic property of electrons.

$$\mu = 2.83 \sqrt{X_{_M}T} \qquad \qquad \mu \text{ is the magnetic moment in Bohr magnetons } \mu_{\text{B}}$$

$$X_{\text{M}} \text{ is the molar susceptibility, } \mu_{\text{B}}{}^2\text{K}^{\text{-}1}$$

T is the temperature, K

73

Magnetism can be thought of (classically) as arising from electron <u>spin</u> and electron <u>orbiting</u> about the nucleus.

The magnetic moment resulting from <u>electron spin</u> is denoted μ_s and is called the **spin-only magnetic moment**.

The moment resulting from the electron $\underline{\text{'orbiting'}}$ the nucleus is the **orbital magnetic moment** denoted μ_l

The μ_s contributes most significantly to the observed magnetic moments, most particularly for first row transition metals.

$$\mu_S = 2\sqrt{S(S+1)}$$
 S = n/2 = total spin quantum number

 μ_S may be estimated by the following equation, where n equals the number of unpaired electrons.

$$\mu_{Spin-only} = \sqrt{n(n+2)}$$

Effective Magnetic Moment - Experimental

 χ_{M} is expressed in Bohr Magnetons (µ_B) where 1 μ_{B} = $\mathit{eh}/4\pi\mathit{m_{e}}$ = $9.27x10^{-24}$ JT $^{-1}$

$$\mu_{eff} = \sqrt{\frac{3k\chi_m T}{L\mu_0 {\mu_B}^2}}$$

where k= Boltzmann constant; L= Avogadro number, $\mu_0=$ vacuum permeability, T= temperature in kelvin

$$\mu_{eff} = 0.7977 \sqrt{\chi_m T}$$
 (in SI units χ_m is in cm^3 / mol)

$$\mu_{eff} = 2.828 \sqrt{\chi_m T}$$
 (in Gaussian units)

75

Effective Magnetic Moments - High Spin First Row

Metal ion	d ⁿ configuration	S	$\mu_{ ext{eff}}(ext{spin-only})/\mu_{ ext{B}}$	Observed values of $\mu_{\rm eff}$ / $\mu_{\rm B}$
Sc ³⁺ , Ti ⁴⁺	d^{0}	0	0	0
Ti ³⁺	d^1	$\frac{1}{2}$	1.73	1.7-1.8
V^{3+}	d^2	1	2.83	2.8-3.1
V^{2+} , Cr^{3+}	d^3	$\frac{3}{2}$	3.87	3.7-3.9
Cr ²⁺ , Mn ³⁺	d^4	2	4.90	4.8-4.9
Mn ²⁺ , Fe ³⁺	d^5	$\frac{5}{2}$	5.92	5.7-6.0
Fe ²⁺ , Co ³⁺	d^6	2	4.90	5.0-5.6
Co ²⁺	d^7	$\frac{3}{2}$	3.87	4.3-5.2
Ni ²⁺	d^8	1	2.83	2.9-3.9
Cu^{2+} Zn^{2+}	d^9	$\frac{1}{2}$	1.73	1.9-2.1
Zn^{2+}	d^{10}	0	0	0

Spin and Orbital Contributions to the Magnetic Moment

Best for lanthanides

 $\left.\begin{array}{ll} \mu_{\rm eff}=g_J\sqrt{J(J+1)}\\ \text{where} & g_J=1+\left(\frac{S(S+1)-L(L+1)+J(J+1)}{2J(J+1)}\right) \end{array}\right\}$

Van Vleck formula, where spin and orbital are independent (1st row)

 $\mu_{\rm eff} = \sqrt{4S(S+1) + L(L+1)}$

No orbital contribution, e.g. (1st row d5)

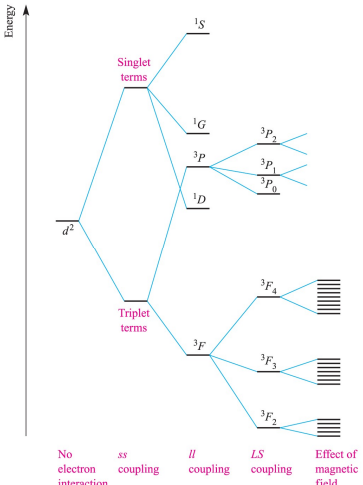
 $\mu_{\mathrm{eff}} = \sqrt{4S(S+1)} = 2\sqrt{S(S+1)}$

Metal ion	Ground term	$\mu_{ m eff}$ / $\mu_{ m B}$ calculated from eq. 20.20	$\mu_{ m eff}$ / $\mu_{ m B}$ calculated from eq. 20.21	$\mu_{ m eff}/\mu_{ m B}$ calculated from eq. 20.22
Ti^{3+}	$^{2}D_{3/2}$	1.55	3.01	1.73
V^{3+}	${}^{3}F_{2}^{5/2}$	1.63	4.49	2.83
V ²⁺ , Cr ³⁺ Cr ²⁺ , Mn ³⁺	$^{4}F_{3/2}$	0.70	5.21	3.87
Cr^{2+} , Mn^{3+}	$^{5}D_{0}$	0	5.50	4.90
Mn^{2+} , Fe^{3+}	$^{6}S_{5/2}$	5.92	5.92	5.92
Fe ²⁺ , Co ³⁺ Co ²⁺	5D_4	6.71	5.50	4.90
Co ²⁺	$^{4}F_{9/2}$	6.63	5.21	3.87
Ni ²⁺	$^{3}F_{4}$	5.59	4.49	2.83
Cu ²⁺	$^{2}D_{5/2}$	3.55	3.01	1.73

77

Spin–orbit coupling coefficients, λ , for selected first row *d*-block metal ions.

Metal ion	Ti^{3+}	V^{3+}	Cr^{3+}	Mn^{3+}	Fe ²⁺	Co ²⁺	Ni ²⁺	Cu^{2+}
d^n configuration	d^1	d^2	d^3	d^4	d^6	d^7	d^{8}	d^9
λ / cm^{-1}	155	105	90	88	-102	-177	-315	-830



Splitting of the terms of a d^2 ion

The constant, λ , dictates the extent of the spin-orbit coupling.

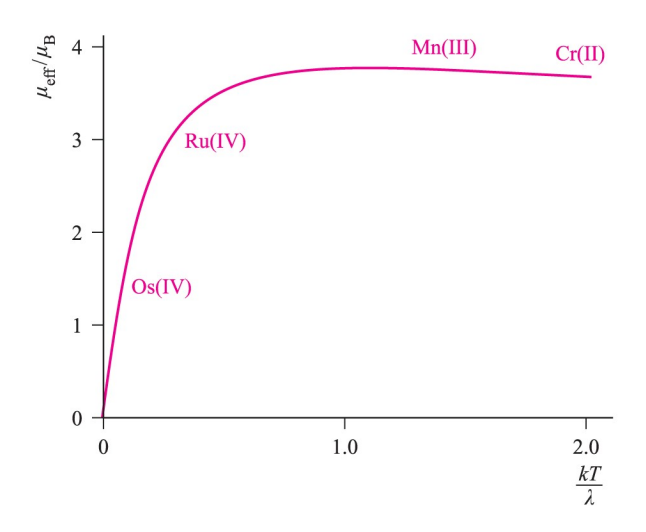
becomes larger for 2nd, 3rd row TM

For ions with A or E ground terms:

$$\mu_{eff} = \sqrt{n(n+2)} \left(1 - \frac{\alpha \lambda}{\Delta_{oct}} \right)$$

Where λ = spin-orbit coupling constant α = 4 for an A ground term α = 2 for an E ground term

Kotani plot for a t_{2g}^{4} configuration



The influence of temperature on μ_{eff} is evident on a Kotani plot.

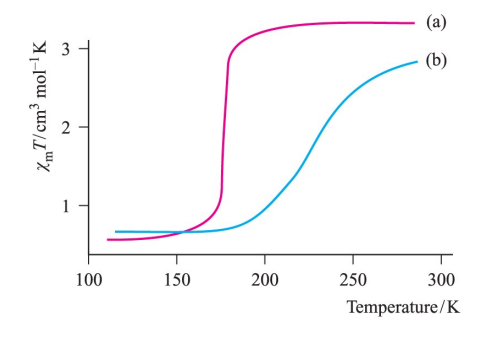
- μ_{eff}(298 K) for first row TM ions lie on near horizontal part of curve, so changing T has small effect on μ_{eff}.
- μ_{eff}(298 K) for heavier TM ions lie on the steep part of curve, so μ_{eff}. is sensitive to changes in T

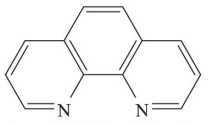
79

spin crossover

Some d⁴,d⁵,d⁶,d⁷ complexes exhibit a spin-crossover transition

• a change in pressure or temperature may induce the transition.



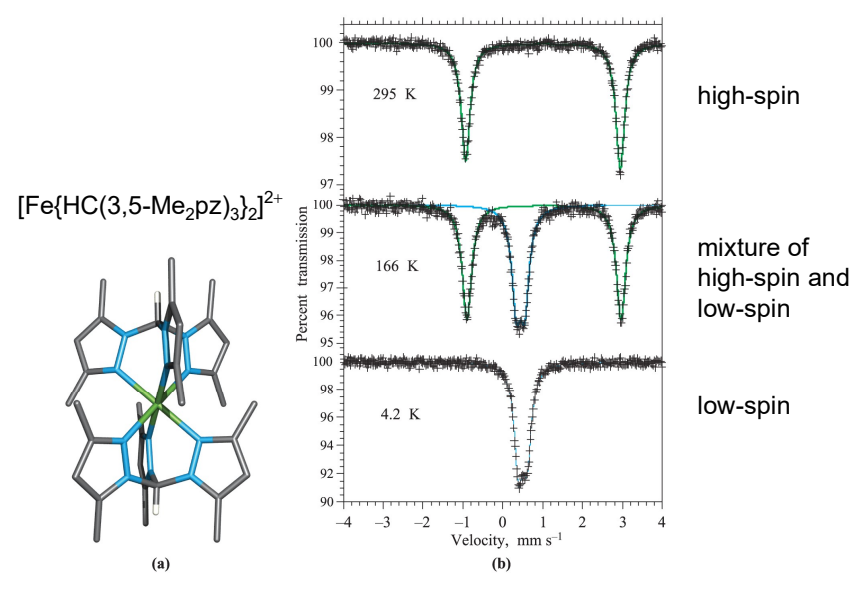


phen = 1,10-phenanthroline

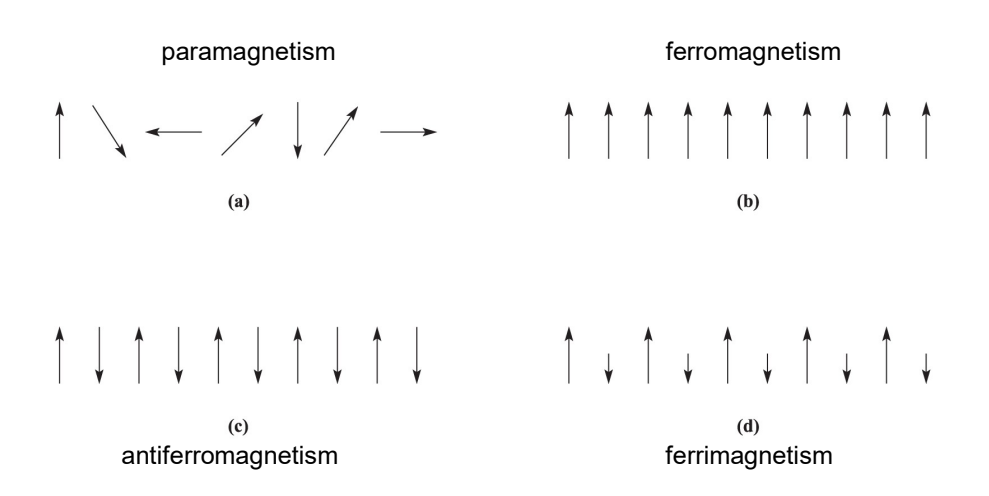
$$\left\langle \begin{array}{c} N \\ S \end{array} \right\rangle \left\langle \begin{array}{c} N \\ S \end{array} \right\rangle$$

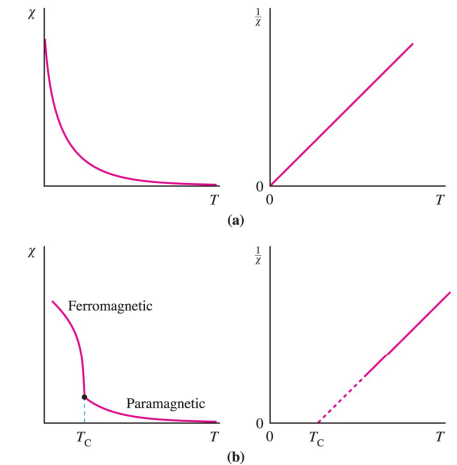
btz = 2,2'-bi-4,5-dihydrothiazine

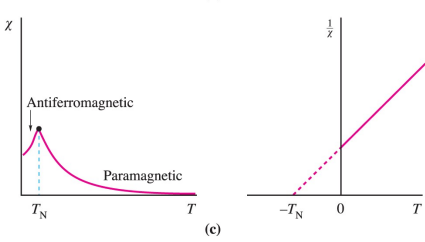
The dependence of the observed values of μ_{eff} on temperature for (a) [Fe(phen)₂(NCS-N)₂] where low- to high-spin crossover occurs abruptly at 175 K, and (b) [Fe(btz)₂(NCS-N)₂] where low- to high-spin crossover occurs more gradually.



Mössbauer spectra of crystallized [Fe{HC(3,5-Me $_2$ pz) $_3$ } $_2$]I $_2$







Curie Law

where C = Curie Constant and T = temperature in K.

$$\chi = \frac{C}{T - T_c}$$

 $\chi = \frac{C}{T}$

Curie-Weiss Law

where C = Curie Constant, T_c = Curie Temperature, and T = temperature in K.

$$\chi = \frac{C}{T - \theta}$$

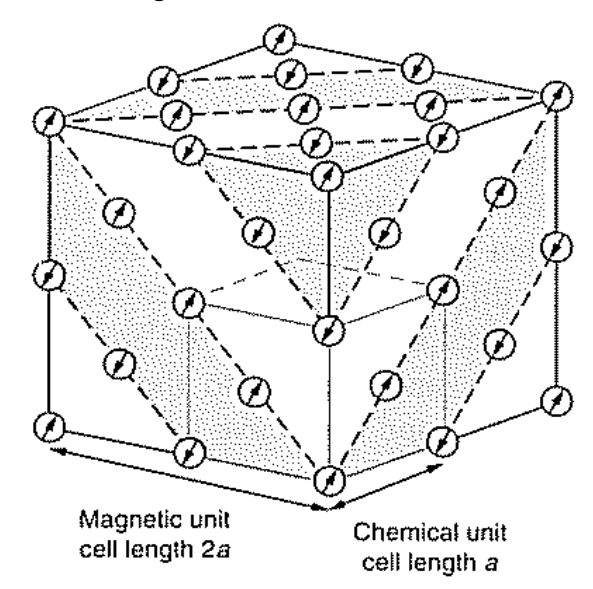
Curie-Weiss Law

where C = Curie Constant, θ = Weiss constant, T = temperature in K, and T_N = Néel temperature.

83

Magnetic unit cell

Neutron diffraction, with a neutron beam that responds to nuclear positions and magnetic moments, is the primary experimental method used to determine the magnetic **structure** of a material.



Consider the magnetic properties of two Fe³⁺ complexes: potassium hexacyanoferrate(III) *and* potassium hexafluoroferrate(III)

$$K_3[Fe(CN)_6]$$
 $K_3[FeF_6]$

Iron(III) is a d^5 ion, capable of both low and high spin states.

These two complexes can be prepared and their magnetic properties measured.

Molar susceptibilities are the following at 25 °C:

$$1.41 \times 10^{-3} \, \mu_B^2 K^{-1}$$
 14.6 x $10^{-3} \, \mu_B^2 K^{-1}$

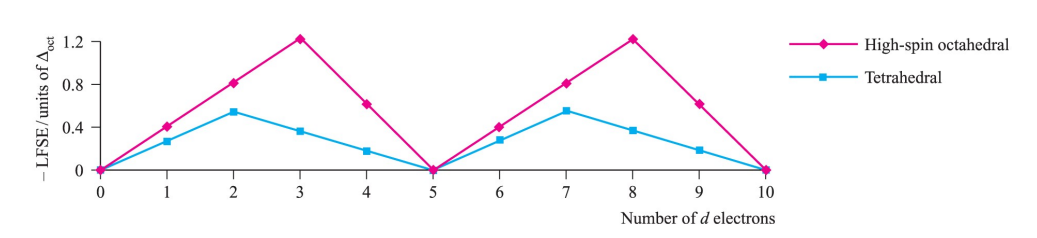
Using $\mu = 2.84\sqrt{X_MT}$ the magnetic moments are:

$$1.84 \, \mu_B$$
 5.92 μ_B

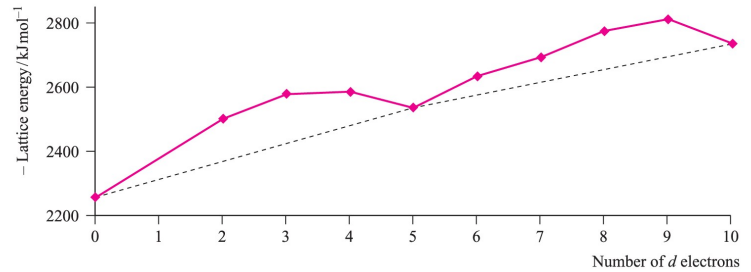
These results are consistent with 1 and 5 unpaired electrons, respectively.

Magnetic measurements may be used to investigate the spectrochemical series.

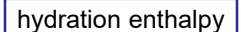
85

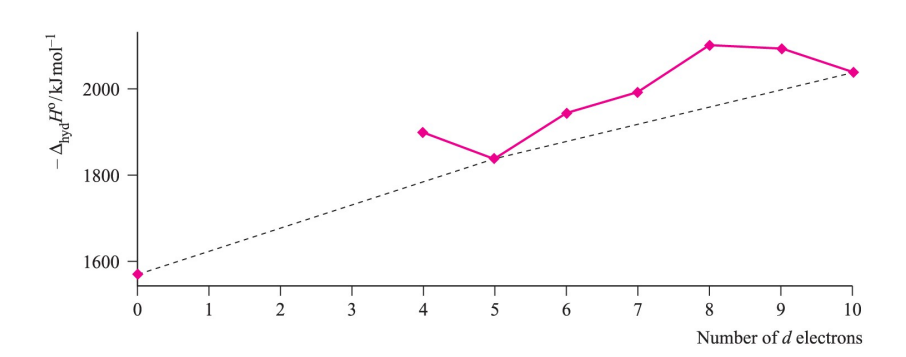


Ligand field stabilization energies as a function of $\Delta_{\rm oct}$ for high-spin octahedral systems and for tetrahedral systems



Lattice energies (derived from Born–Haber cycle data) for MCl₂ where M is a first row *d*-block metal





General and similar trends are found between LFSE and the enthalpies of hydration of the M^{2^+} ions of the first row metals.

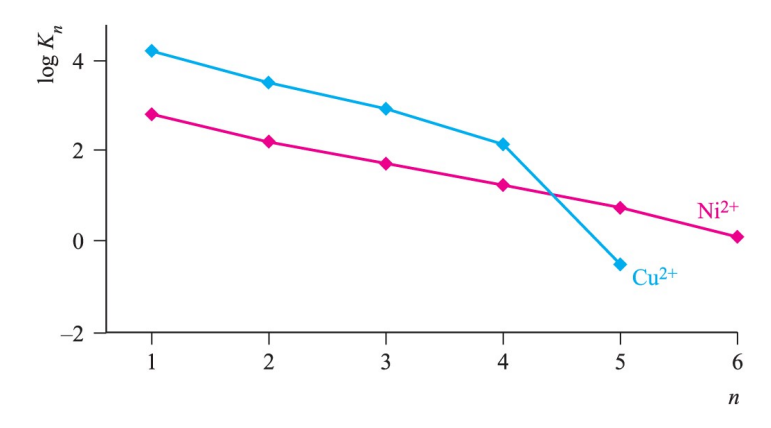
- Only part of the measured hydration enthalpy can be attributed to the first coordination sphere of the 6 H₂O molecules.
- LFSE is not the only factor in total interaction energies, it is merely an approximation and has some uses.

87

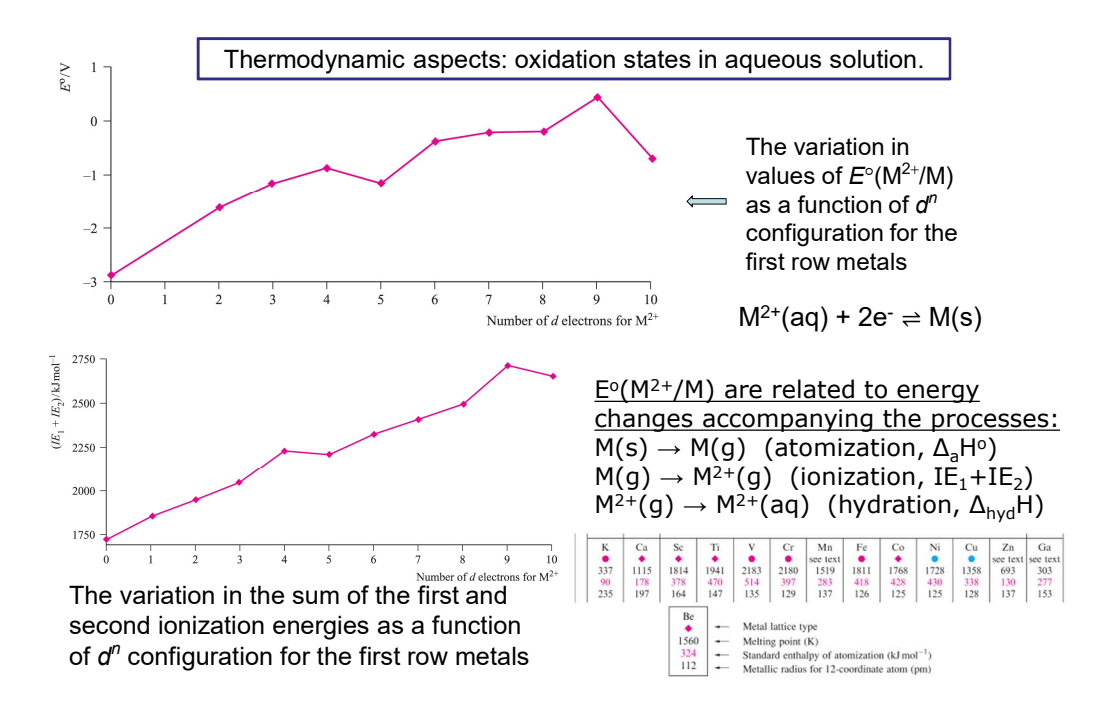
		Irving-Williams	<u> </u>
Iharmadi	mamic achacte	Irvina Williame	Sarias
HIIGHIOO	ขาสเมเน สอบธนเอ.	. II vii iu-vviiliai iis	OCHES.
	,		

Metal ion	Mn^{2+}	Fe ²⁺	Co ²⁺	Ni ²⁺	Cu^{2+}	Zn^{2+}
$log\beta_3 for [M(en)_3]^{2+}$	5.7	9.5	13.8	18.6	18.7	12.1
$\log \beta$ for $[M(EDTA)]^{2-}$	13.8	14.3	16.3	18.6	18.7	16.1

Overall stability constants for selected high-spin *d*-block metal complexes.



Stepwise stability constants (log K_n) for the displacement of H_2O by NH_3 from $[Ni(OH_2)_6]^{2+}$ (d^8) and $[Cu(OH_2)_6]^{2+}$ (d^9).



LFSE has a minimal influence on standard reduction potential

89

Standard reduction potentials for the equilibrium $M^{3+}(aq) + e^- \rightleftharpoons M^{2+}(aq)$ and values of the third ionization energies.

M	V	Cr	Mn	Fe	Co
E° / V	-0.26	-0.41	+1.54	+0.77	+1.92
$IE_3/\mathrm{kJ}\;\mathrm{mol}^{-1}$	2827	2992	3252	2962	3232

In general, a larger value of IE_3 corresponds to a more positive E° value.

 This suggests a steady increase difference in the hydration energies between M³⁺ and M²⁺ (hydration energy becomes larger as ions become smaller) is outweighed by the variation in IE₃.

Examine IE_3 and E° vanadium and chromium and explain the observed trend. Assuming hexaaqua metal complexes, consider the change in electronic configuration and Δ LFSE.

